


AN ABSTRACT OF THE THESIS OF

Philip Arthur Jarvis for the M.S. in Mechanical Engineering  
(Name) (Degree) (Major)

Date thesis is presented May 11, 1966

Title DEVELOPMENT OF A METHOD TO DETERMINE THE  
PENETRATION VELOCITY OF A POWDER ACTUATED FASTENER

Abstract approved 

The purpose of this work was to design a system for measuring the velocity of a powder actuated fastener or drivepin during penetration. This system would provide a tool for further investigation into drivepin penetration characteristics. The main characteristic of interest is the instantaneous acceleration from which the forces on the drivepin can be determined. This acceleration was determined by designing a transducer whose output is drivepin position versus time and calculating the instantaneous velocity and acceleration, graphically and numerically, from these data.

A powder actuated drivepin is a special nail-like pin which is driven into hard materials by the force of a charge of gunpowder. The powder actuated tool is similar to a pistol except the projectile is the drivepin and the charge is in a separate brass jacket. The penetration velocity previously referred to is the velocity spectrum during the total time the drivepin is in motion.

Some of the transducers that were considered are listed with comments which affected their evaluation. Among these transducers, the linear resistance potentiometer was selected for this measuring system. It has the following characteristics:

- a. Simplicity
- b. High frequency response
- c. Good linearity
- d. Marginal mechanical strength
- e. Low, but sufficient output

With this potentiometric transducer, an oscilloscope and camera were added to provide a time base and a permanent record.

The test results or data are recorded as photographs of the oscilloscope trace. Various techniques for differentiating these data are discussed. These techniques include graphical, approximating polynomials by the method of finite differences, and best fitting curve by the method of least squares.

Additional mathematical presentations are included to show the measuring system's linearity and frequency response and the equations of motion of the powder actuated tool and piston.

The final configuration of the measuring system is a battery energized slide wire mounted inside a barrel and a collector mounted opposite the slide wire. The head of the drivepin contacts the slide wire during penetration and transfers this voltage to the

collector. The collector voltage is fed into an oscilloscope for display as a function of time. The external trigger signal for starting the display is obtained from the first motion of drivepin as it passes through a metal foil on the surface of the material to be penetrated.

This potentiometric measuring system was found to be adequate for the purpose intended. However, some mechanical modifications are recommended.

DEVELOPMENT OF A METHOD TO DETERMINE THE  
PENETRATION VELOCITY OF A POWDER ACTUATED FASTENER

by

PHILIP ARTHUR JARVIS

A THESIS

submitted to

OREGON STATE UNIVERSITY

in partial fulfillment of  
the requirements for the  
degree of

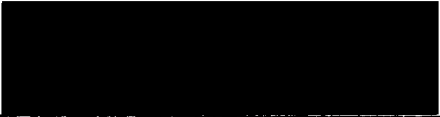
MASTER OF SCIENCE

June 1966

APPROVED:

  
\_\_\_\_\_  
Professor of Mechanical Engineering

In Charge of Major

  
\_\_\_\_\_  
Head of Mechanical Engineering Department

  
\_\_\_\_\_  
Dean of Graduate School

Date thesis is presented 11 May 66

Typed by Gail Dailey

## ACKNOWLEDGMENT

The author wishes to acknowledge the contribution of Omark Industries, Inc. and to express his appreciation for the advice received from Earl Sutherland, Myron Tupper, and Joe Van Gulik of that company. He especially wishes to thank Professor Wesley W. Smith of Oregon State University for his personal counsel and encouragement.

## TABLE OF CONTENTS

	<u>Page</u>
I INTRODUCTION	1
II PRELIMINARY INVESTIGATION	8
Prior Related Work	8
Transducers	9
Non-Contacting Transducers	10
Contacting Transducers	12
III TEST METHOD AND INSTRUMENTATION	19
IV EXPERIMENTAL RESULTS	26
Test A	27
Test B	34
Test C	41
Test D	47
Test E	52
Test F	58
V DISCUSSION OF TEST RESULTS	64
VI CONCLUSIONS AND RECOMMENDATIONS	80
BIBLIOGRAPHY	82
APPENDICES	83
Appendix I	83
Appendix II	93
Appendix III	99
Appendix IV	100
Appendix V	101
Appendix VI	102
Appendix VII	103
Appendix VIII	104

## LIST OF FIGURES

	<u>Page</u>
1. Typical powder actuated tools and drivepins	4
2. Typical drivepins and powder loads	5
3. Powder actuated tool, transducer, and power plug	6
4. Potentiometer with true constant current source	18
5. Potentiometer with pseudo constant current source	18
6. Transducer 20-1-D output vs. pin position	23
7. Transducer 20-1-F output vs. pin position	24
8. Transducer 20-1-G output vs. pin position	25
9. Transducer 20-1-C	29
10. Transducer 20-1-D and 20-1-F	29
11. Piston 20-4-3-A	29
12. Test circuits 1 and 2	31
13. Test circuits 3 and 4	31
14. Wiper and pin assembly	32
15. Transducer output, Test A-1	33
16. Transducer output, Test B-1	35
17. Transducer output, Test B-2	35
18. Transducer output, Test B-3	37
19. Transducer output, Test B-4	37
20. Resistance elements and collectors 20-2	39
21. Transducer output, Test C-2	44
22. Transducer output, Test C-2	44



	<u>Page</u>
23. Transducer output, Test C-3	45
24. Transducer output, Test C-4	45
25. Test C	46
26. Transducer output, Test D-1	49
27. Transducer output, Test D-2	49
28. Test D	50
29. Resistance element and damaged collector 20-2-E	51
30. Transducer 20-1-G	53
31. Test circuits 5 and 6	55
32. Transducer output, Test E-1	56
33. Transducer output, Test E-2	56
34. Transducer output, Test F-1	59
35. Transducer output, Test F-2	59
36. Damaged resistance element 20-2-1-F	60
37. Damaged collector 20-5	61
38. Variation of source current with time	66
39. Penetration velocity vs. time	71
40. Collector 20-5	72

## LIST OF APPENDIX FIGURES

	<u>Page</u>
1. Potentiometer circuit	84
2. Simplified potentiometer circuit	85
3. Simplified transducer impedance	85
4. Thévenin's equivalent circuit	86
5. Oscilloscope input impedance	86
6. Powder actuated tool and piston	94
7. Free body diagram of the tool	94
8. Free body diagram of the piston	94

## DEFINITIONS, SYMBOLS AND ABBREVIATIONS

-A = Change letter for thesis drawing

Av. = Average

-B = Change letter for thesis drawing

-C = Change letter for thesis drawing

C = Capacitance in farads

Calib. Vert. Sens. = Calibrated vertical sensitivity obtained from the  
oscilloscope vertical scale factor in mv/div and  
the transducer output mv/inch of pin travel

Dist. = Distance pin travelled

div = Divisions from the scope graticule

D/N = Drawing Number

Drivepin = powder actuated fastener or pin

e = Base of the Natural Logarithm

e(s) = Laplace Transform of E(t)

E(t) = E which is a function of t

FPM = Feet per minute

FPS = Feet per second

f(s) = Laplace transform of F(t)

F(t) = F which is a function of t

Graticule = the x-y grid on the face of the oscilloscope

H1 = Height of the top of drivepin from surface of the workpiece  
before firing

H2 = Height of the top of the drivepin from the surface of the work-  
piece after firing

H2 - H1 = Depth of pin penetration as measured by the length of  
pin-head travel

Hor. = Horizontal

Hor. Sens. = Horizontal sensitivity from oscilloscope  $\frac{\text{millisec}}{\text{x division}}$

IPS = Inches per second

In. = Inch, inches

KE = Kinetic energy

$L[F(t)]$  = Laplace transform of  $F(t)$

Millisec. = milliseconds

Mult. = Multiplier

ms = Millisecond

mv = millivolts

N. A. = Not available

Nom. = Nominal

P. A. T. = powder actuated tool

Pin = drivepin or fastener

P/N = Part number, Omark

psi = Pounds per square inch

s = Laplace variable

Scope = Oscilloscope

Sens. = Sensitivity

Sens. Mult. = Sensitivity Multiplier

$$= \frac{\text{Vertical Sensitivity}}{\text{Horizontal Sensitivity}} \text{ of oscilloscope}$$

Slide wire = Used as synonym for resistance element

S/N = Serial number

t = Time

$$\text{Tan} = \text{Tangent} = \frac{\text{y division}}{\text{x division}}$$

Time of Penetration = Time drivepin is in motion

Tool = Powder actuated tool

Tophet C = Nickel-Chrome resistance ribbon manufactured by Wilbur  
B. Driver Co.

Total Distance = Total distance of pin travel as calculated from the  
area under the velocity-time curve. That is, the  
average velocity multiplied by the time that velocity  
acts.

Trace = Oscilloscope trace or display

Vel = Velocity

Vert. = Vertical

Vertical Scale Factor = Oscilloscope vertical sensitivity (mv/div)

$$\text{Vert. Sens.} = \text{Vertical Sensitivity} = \frac{H1 - H2}{x1 - x2} \frac{\text{inches}}{\text{division}}$$

= Vertical sensitivity obtained di-  
rectly from trace and measured  
penetration of the drivepin

Workpiece = that material into which the pin is driven - usually  
concrete or steel

x = Scope abscissa (origin at center - positive to the right)

y = Scope ordinate (origin at center - positive upward)

y1 = Ordinate of the scope trace before firing

y2 = Ordinate of the scope trace after firing

20-1)

-2) Thesis Drawing Numbers

-3)

20-1-A)

-B) Drawing Change Numbers

-C)

$\Delta$  = Delta = Change in distance

$\theta$  = Average slope in degrees

# DEVELOPMENT OF A METHOD TO DETERMINE THE PENETRATION VELOCITY OF A POWDER ACTUATED FASTENER

## I. INTRODUCTION

A powder actuated fastener or drivepin is a special nail-like pin which is driven into concrete or steel by the force of a charge of gunpowder. The tool used to drive these pins is essentially a pistol with semi-fixed ammunition (separate shell and projectile). The shell is called a jacketed power load or "load" and the projectile is a hardened steel drivepin.

The drivepin is accelerated from a rest position in the barrel to a finite velocity and decelerates to a stop while penetrating hard material. For the majority of drivepin applications, this hard material is concrete and, consequently, it is very difficult to predict the resistance to the drivepin travel. This resistance to penetration may be a function of the strength of concrete, the size, location, and strength of aggregate and angle of attack of the drivepin. Hence, in order to determine the actual forces on a drivepin, a method was needed for determining the drivepin acceleration and deceleration for a large number of firings. After considering various methods of determining the drivepin accelerations, a method of measuring the velocity spectrum or velocity at every instant during penetration was selected to yield data so the drivepin accelerations can be determined by calculation.

The development of a method for the determination of the drivepin acceleration (plus or minus) during the time it enters the workpiece is desired so that it may be used for future investigations concerning

1. forces on the drivepin
2. velocity-penetration relationships.

This last item was the most prominent reason for developing this measuring system.

The tools for driving these pins are of two kinds:

1. Those whose fastener is driven by the direct action of the explosive charge. (High Velocity Tools)
2. Those whose fastener is driven by a piston which is in turn propelled by the explosive. (Low Velocity Tools)

Typical tools and drivepins and loads are shown in Figures 1 and 2.

The energy of the load in the high velocity tool is transferred into kinetic energy of the drivepin. The energy of the load of a low velocity tool, on the other hand, is transferred into kinetic energy of the drivepin and the piston, which reduces the velocity of the pin.

This reduction in drivepin initial velocity can be shown by assuming that the load energy (neglecting losses) must equal the



kinetic energy of the moving masses. For the high velocity tools

$$KE = 1/2mV^2$$

where

m = mass of the drivepin

V = velocity of the high velocity drivepin

and, for the low velocity tools

$$KE = 1/2(m + M)v^2$$

where

M = mass of the piston (roughly 15 times the mass of the drivepin)

v = velocity of the low velocity drivepin.

Therefore, since

$$1/2mV^2 = 1/2(m + M)v^2$$

or

$$\frac{V}{v} = \sqrt{\frac{M+m}{m}} \approx \sqrt{\frac{15+1}{1}} \approx 4$$

Thus, for the same powder load, the drivepin velocity from the high velocity type tool will be roughly four times that of pins from the low velocity type tool.

A low velocity tool was selected for this work for convenience and safety. See Figure 3. However, the actual measuring method developed is applicable to both types of tools.

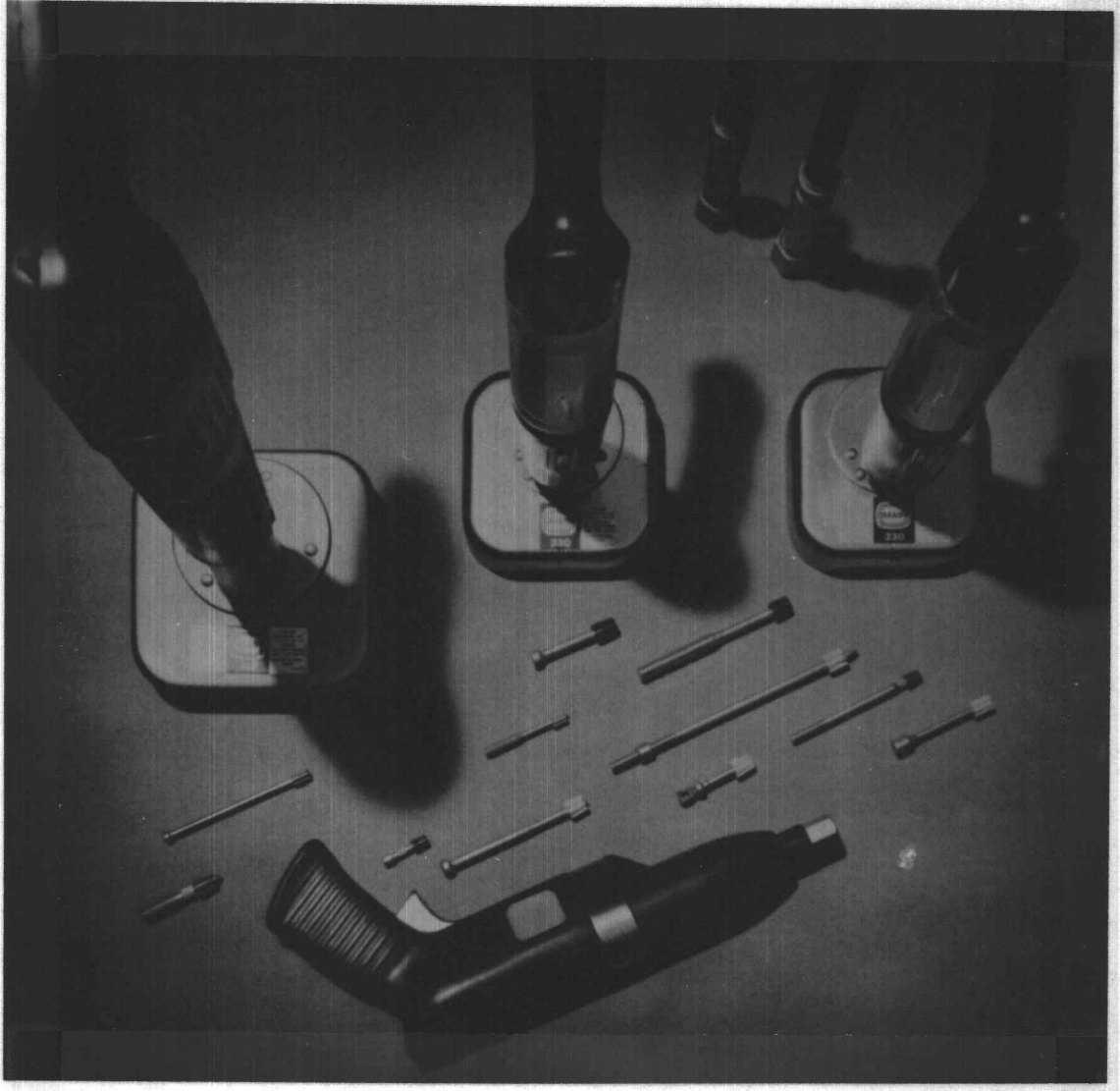


Figure 1. Typical powder actuated tools and drivepins.

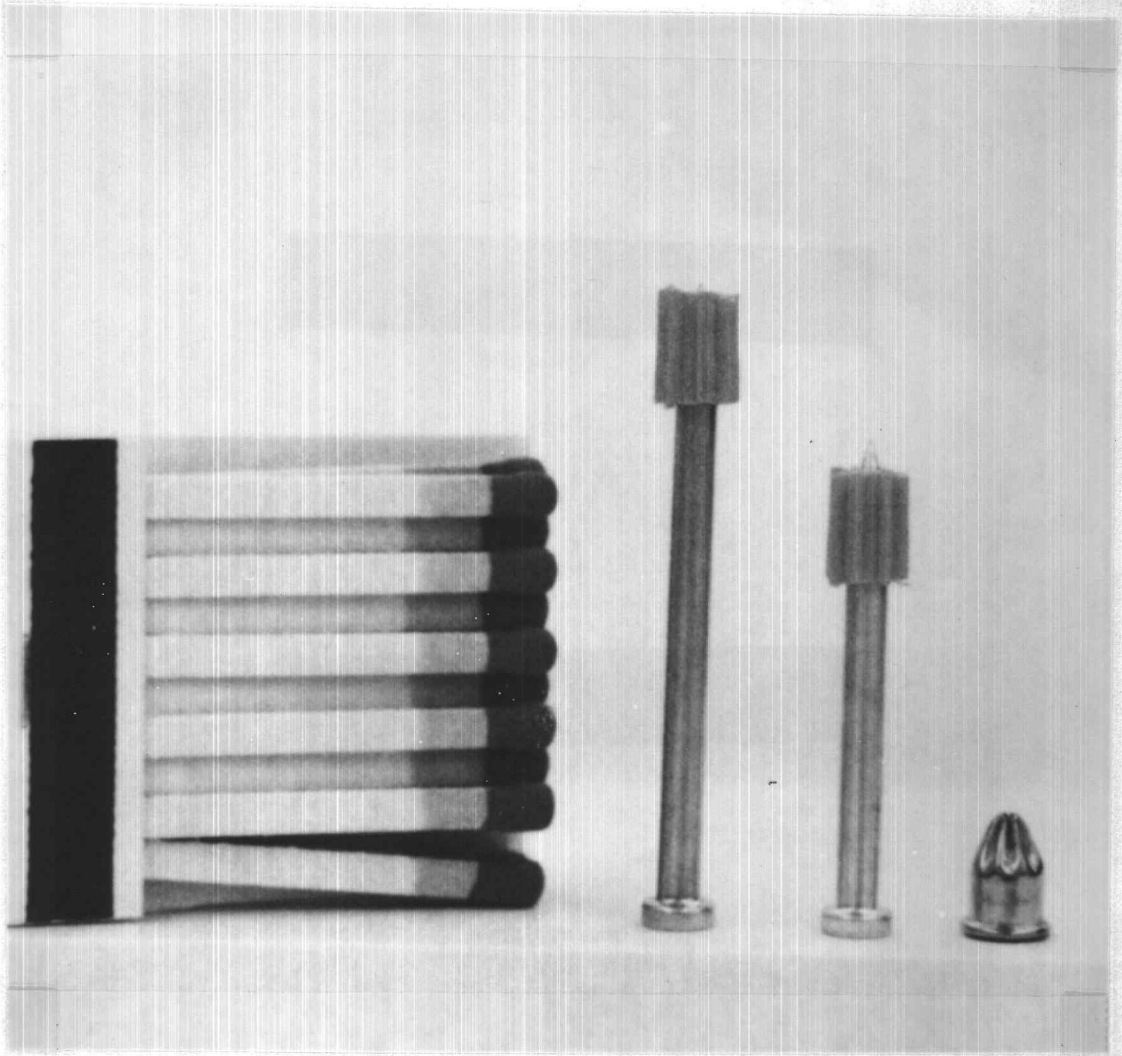


Figure 2. Typical drivepins and powder loads.



Figure 3. Powder actuated tool, transducer, and power plug.

The overall approach was to search the literature for previous related work and for possible methods which could be used, to reduce the possible methods to one, then to turn this method into hardware, test, modify hardware as required, retest, and report.

In searching for a suitable method of obtaining the penetration velocities the following requirements were considered important:

1. The method must measure and record the velocity continuously as the drivepin is in motion or, at least, determine its average velocity for sufficiently small increments of time.
2. The method should not require special treatment of the drivepin since the drivepin can be used only once.
3. The method should be adaptable to high velocity as well as low velocity tools.
4. The method should be as simple and the measuring system as rugged as possible.

The following section lists various methods which could be used to obtain the required velocity information, how they could be used, their properties, and the factors which influenced the selection of the method chosen.

## II. PRELIMINARY INVESTIGATION

### Prior Related Work

This investigation concentrated on locating prior related work in the literature and investigating several measuring methods or transducers which could possibly be utilized.

The only directly applicable paper on drivepin velocities was by Dr. H. D. Seghezzi \* entitled "A Study of Kinetic Energy as a Cause of Accident Hazards with Powder Actuated Tools." Seghezzi mentioned only that the velocity of the drivepin during penetration was measured by means of a high speed film record. He does not elaborate. Other points of interest from this article are: the total time of penetration varies from 0.1 to 2 milliseconds, that free flight velocities of piston type tools range from 200 to 300 feet per second, and maximum velocity during penetration into 1/4" steel was 278 feet per second. He mentions free flight velocities as measured by a standard light beam interruption system. This method is quite common and most of the velocity data available are of this type. However, this method measures the constant velocity over a given distance (from five feet to eight feet from the muzzle) and is not applicable for measuring instantaneous or continuous penetration velocities. The general tone of the article, however,

---

\* Translated from the Austrian Magazine "Sichere Arbeit" (Safety Work) Volume 17, 1964.

was concerning safety. The high speed film technique will be discussed at greater length later in this section.

### Transducers

A transducer is a device which transforms one form of energy into another. The various transducers considered for determining the instantaneous velocity during penetration can be divided into two categories:

1. Those which require no mechanical contact with the drivepin
  - a. Linear differential transformer
  - b. Variable reluctance pickoff (magnetic)
  - c. Variable capacitance pickoff
  - d. Optical methods (Cameras)
  - e. X-ray methods.
2. Those which require mechanical contact with the drivepin
  - a. Mechanically actuating a switch with the head of the drivepin.
  - b. Placing a linear potentiometer in the barrel and using the drivepin as a wiper.

## Non-Contacting Transducers

Linear Differential Transformer. The differential transformer is an electromechanical transducer that generates an output voltage proportional to the displacement of a movable core. The core, the drivepin for this application, provides a path for the magnetic lines of force linking the primary and the secondary, and since the two secondary coils are wound in series opposition at opposite ends of the transducer, the output is zero when the core is centered. This is because the flux linking each secondary coil is equal. The output is linear only for limited displacements of the core on either side of the null position.

This transducer was not considered for the following reasons:

1. Lack of linear output throughout the drivepin travel.
2. Difficulties which may occur in using a drivepin instead of a special cylindrical ferromagnetic core.
3. Limited frequency response. The maximum recommended frequency is 10 percent of the primary excitation frequency (7, p. 4).
4. Difficulties which may occur because of the presence of the piston.



Variable Reluctance Pickoff. An array of 24 variable reluctance pickoffs could be mounted on a barrel extension. These pickoffs generate a voltage whenever the magnetic field near the pole piece is disturbed. Thus, the head of the pin will cause a pulse to be generated as it passes by the pole piece. Unfortunately, the magnitude of this pulse is a function of the pin velocity.

This transducer was not used for the following reasons:

1. The magnitude of the output is a function of the drivepin velocity.
2. The presence of the magnetic piston presents special problems.
3. The frequency response of the circuit is doubtful due to the inductive elements.

Variable Capacitance Pickoff. The capacitance method of measuring pin position was not considered because of the requirement of ac energization of the transducer and the need for a frequency sensitive discriminator to convert the change in capacitance to a change in voltage for display on an oscilloscope.

Optical Methods--High Speed Cameras. Stopping the motion of the drivepin with a high speed movie camera was considered. Investigation of available equipment revealed that the highest frame

rate was 16,000 frames per second with a Fastex #WF2. However, the penetration occurs in less than one millisecond so this camera speed would yield less than 16 exposures per shot.

This method was discounted for the following reasons:

1. The requirement for an optical path through the barrel.
2. The difficulty in determining the actual film speed. An external time reference should be included in each exposure.
3. The lack of continuous position versus time information.

X-ray Methods. Multiple flash X-ray technique was considered and rejected for the following reasons:

1. Radiation hazard
2. Complexity and expense of the X-ray equipment.
3. Limited number of X-ray pulses available. This small number would not provide the required resolution.

#### Contacting Transducers

Mechanically Actuated Switch. The head of the drivepin could be used to actuate a subminiature switch. As the pin travels

down the barrel, the head strikes a ball which moves a spacer to close the switch. These switches can be mounted as close as .050 inch between centers, however, the head thickness (.070 inch) could cause two switches to be closed at the same time.

This method was not used because of the difficulty in conditioning the pulse type data to make it usable for further calculations.

Potentiometric. A linear potentiometer is an electromechanical device that develops an output proportional to some mechanical input. The resistance potentiometer consists of a battery energized resistance element or slide wire and a movable slider or wiper. The electrical schematic of a potentiometer is shown in Figure 4. The voltage between either end of the resistance element and the wiper is a function of the wiper position.

The different types of resistance elements available are (1):

1. Slide wire (a length of conducting wire).
2. Wirewound (resistance wire helically wound on a mandrel).
3. Carbon film (deposited film on plastic).
4. Metal film (deposited film on plastic).
5. Conductive plastic (deposited film on plastic).
6. Cermet (glass material combined with noble metals on a base).
7. Liquid (electrolytic).

Of these, the simplest and easiest to use for this application is the slide wire, which has the advantages of:

1. Stepless output (infinite resolution).
2. Minimum reactance.
3. Low cost.
4. Relatively high mechanical strength.

The advantage of minimum reactance is important when considering the dynamic response. The greater the reactance, the less able the circuit is to respond linearly to high frequency phenomena.

The major limit to its usefulness is its low maximum resistance. The low resistance of large cross section elements and the larger cross section required for strength, force a compromise in the selection of resistance element material and geometry. That is, the resistance must be high enough to yield sufficient IR drop (output) and still have mechanical strength. If R is low, I can be increased, but only to an allowable  $I^2R$  power dissipation. This allowable power dissipation is governed by the heat transfer characteristics of the circuit.

Noise or unwanted signals are present to some degree in every potentiometer application. Two types of "passive" noise may be encountered in a slide wire potentiometer: vibrational noise, and residual noise from several sources. Vibrational noise is purely mechanical in cause and is produced by the wiper jumping away from

the resistance element and thereby opening the wiper circuit. Wiper geometry and contact pressure can be adjusted to minimize this noise. There are, however, residual noise effects which consist of sharp random voltage peaks generated between the moving contact surface and the slide wire. The principal cause of residual noise is foreign material, so effort should be made to keep the slide wire clean. The amount of oil and unburned residue in a powder actuated tool is great so the bore should be wiped clean after each firing.

The total sources of "active" residual noise usually do not generate more than a small fraction of a millivolt in a standard wire-wound potentiometer. Active noise is self-generated voltage under three principal sets of conditions: galvanic or chemical action at the point of contact between the slide wire and wiper, thermoconductive effects which depend on friction or external heat, and triboelectrical phenomena, small voltages generated by abrasion of the wiper on the slide wire (1).

For this application, however, the actual magnitude of the active noise should be investigated. It could be done by firing the drivepin through the transducer with the battery disconnected and recording the response.

There are three common circuits for this type of potentiometric application:

1. True constant current source. See Figure 4.

2. Pseudo constant current source. See Figure 5. Loading the slide wire by drawing current through the wiper circuit affects the output voltage or linearity, depending on the position of the wiper. A linear potentiometer's output is a linear function of its position only if it is supplied by a constant current source or draws no wiper current. This can be seen intuitively by considering Figure 4. If  $I_C$  is from a constant current source or  $I_L = 0$ , the output voltage will be a linear function of  $R_1$ . Actually, the output voltage varies with the wiper position because there is a current in the wiper circuit. The effect of a finite load is shown in Appendix 1.
3. Basic bridge circuit. The bridge circuit output is not linear for large changes in resistance so it was not considered further.

The pseudo constant current circuit was selected because of its inherent linearity and simplicity.

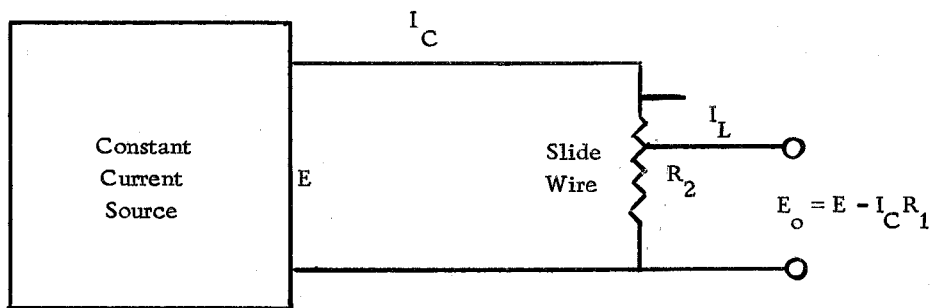
The basic configuration of the test transducer, then, is a battery-supplied resistance element or slide wire mounted inside a barrel and a collector mounted opposite the slide wire. The construction of the resistance element is similar to a beam on an elastic foundation. Timoshenko (10, vol. 2, p. 1-6) develops the equation for an elastic curve which shows the force-deflection relationship for this

method of mounting the resistance element. The drivepin acts as a wiper contacting the slide wire and transferring this voltage to the collector. This voltage is fed into an oscilloscope for display as a function of time and a photograph is taken of the trace.

This transducer is designed to fasten to the end of the barrel of a standard Omark Type 110 low velocity tool in the same manner as a "barrel nut." The length of the transducer is the same as a standard "two inch barrel extension" so the standard pistons can be used.

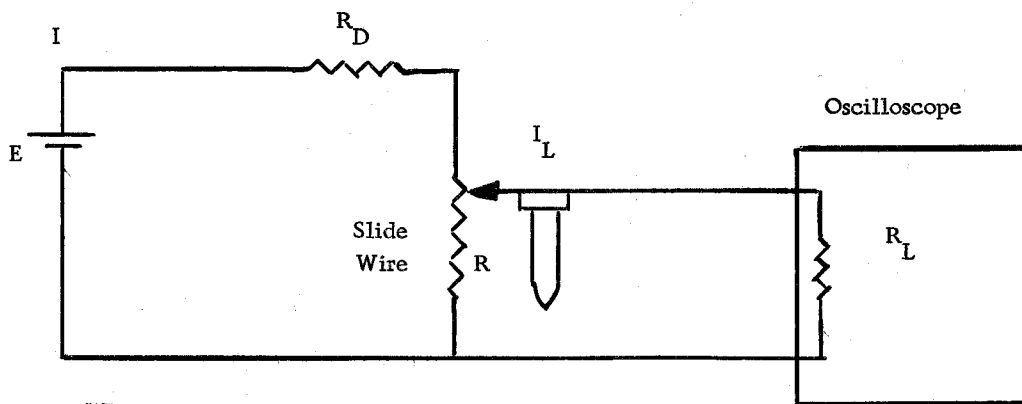
The powder actuated tool, transducer, and the power plug are shown in Figure 3. The power plug slips into the barrel from the breach and serves as the chamber for the gasses of the load. It also contains the piston which drives the fastener into the workpiece. The power plug is easily removable from the barrel so that the jacket from the spent load can be ejected, the piston positioned, and a new load inserted.

This tool and transducer are the subject of the following sections.



$I_L$  Changes with wiper position

Figure 4. Potentiometer with true constant current source



Where  $R_D$  is much greater than R

Note: If  $R_L$  is large enough,  $I_L$  will be negligible and this circuit may be considered a constant current circuit

Figure 5. Potentiometer with pseudo constant current source



### III. TEST METHOD AND INSTRUMENTATION

The ideal method of calibrating a transducer is to excite the transducer with a known input which is identical to the input to be measured and compare the output with this known input. However, the nature of the input for this transducer is not known, so the determination of its ability to measure the velocity spectrum was accomplished by actual firings into the workpiece to show that an output can be obtained and calculating the transducer's linearity and frequency response. See Appendix I. Concerning this response, the specifications of the Tektronix Type CA plug-in with a Type 536 oscilloscope indicate that the rise time is  $35 \times 10^{-9}$  seconds. This is 300,000 times greater than the penetration time. This is more than adequate response.

The tests are arranged in chronological order and show the problems that occurred and how they were corrected or minimized. These tests were aimed at showing that the velocity information can be reliably obtained.

During these tests, observation showed that the tool itself had a velocity relative to the workpiece. Since the transducer measures the pin position relative to the tool, Tests E and F were done to determine when the tool velocity occurs--during or after the drivepin motion.

The constant current potentiometer test circuits and instrumentation for the tests are shown in detail in section IV. The test procedure was as follows:

1. Turn on power.
2. Put load in power plug, piston touching the load.
3. Insert power plug in tool.
4. Put pin in tool from the muzzle.
5. Check initial deflection,  $y_1$ , on the oscilloscope.
6. Short tool to trigger foil to check trigger operation  
(for Tests C, D, E, and F).
7. Push single sweep Reset on the oscilloscope.
8. Depress tool to firing position.
9. Open camera shutter.
10. Fire the tool.
11. Close camera shutter.
12. Extract polaroid print from camera.

The instrumentation included an oscilloscope (single or dual beam depending on the test requirements) and a polaroid oscilloscope camera. The oscilloscope provided a time base and displayed the output voltage of the potentiometer as a function of time. The sweep was programmed to wait until the pin moved before starting the display. This displayed the transducer output as a function of time starting with the initial pin motion.

The most desirable test required the firing of a drivepin of a length such that all the penetration would take place without the drivepin head leaving the barrel. This would allow the camera to record the initial position (voltage), the position versus time of penetration, and the final position. The single triggered sweep provides a stationary spot at the left margin of the graticule as it waits for the trigger or reset. This information, along with the measurement of pin penetration and the assumption of linearity, are sufficient to determine the drivepin position versus time of penetration. The measurements of the initial and final heights of the drivepin head yield a measure of the distance that corresponds to the number of graticule divisions between  $y_1$  and  $y_2$ . The sweep sensitivity gives the time per division. Therefore, the observed vertical division times the inches per division yield inches and the observed horizontal division times time per division yield time.

If, however, the drivepin leaves the barrel, then prior transducer calibration and the oscilloscope vertical sensitivity are required to determine the depth of penetration.

Since the oscilloscope camera is held open for this single sweep, the display from the cathode ray tube is retained on film.

The Nickel-Cadmium batteries for the transducer were selected for their high current capacity, good voltage regulation, and their low nominal voltage. This low voltage is required to avoid dropping

the voltage across an external resistor to obtain the proper current in the resistance element. The dropping resistor wastes power and varies the circuit current due to its change in resistance from heating.

The linearity of the resistance elements for Tests B through F was determined by measuring the output voltage of the transducer as a function of pin position and plotting these data. See Figures 6, 7, and 8. The effect of a finite load was eliminated by using an Electro Scientific Industries PVB 300 bridge. The pin position was determined by forcing the pin into the transducer in 0.100 inch increments with a depth micrometer or vernier caliper.

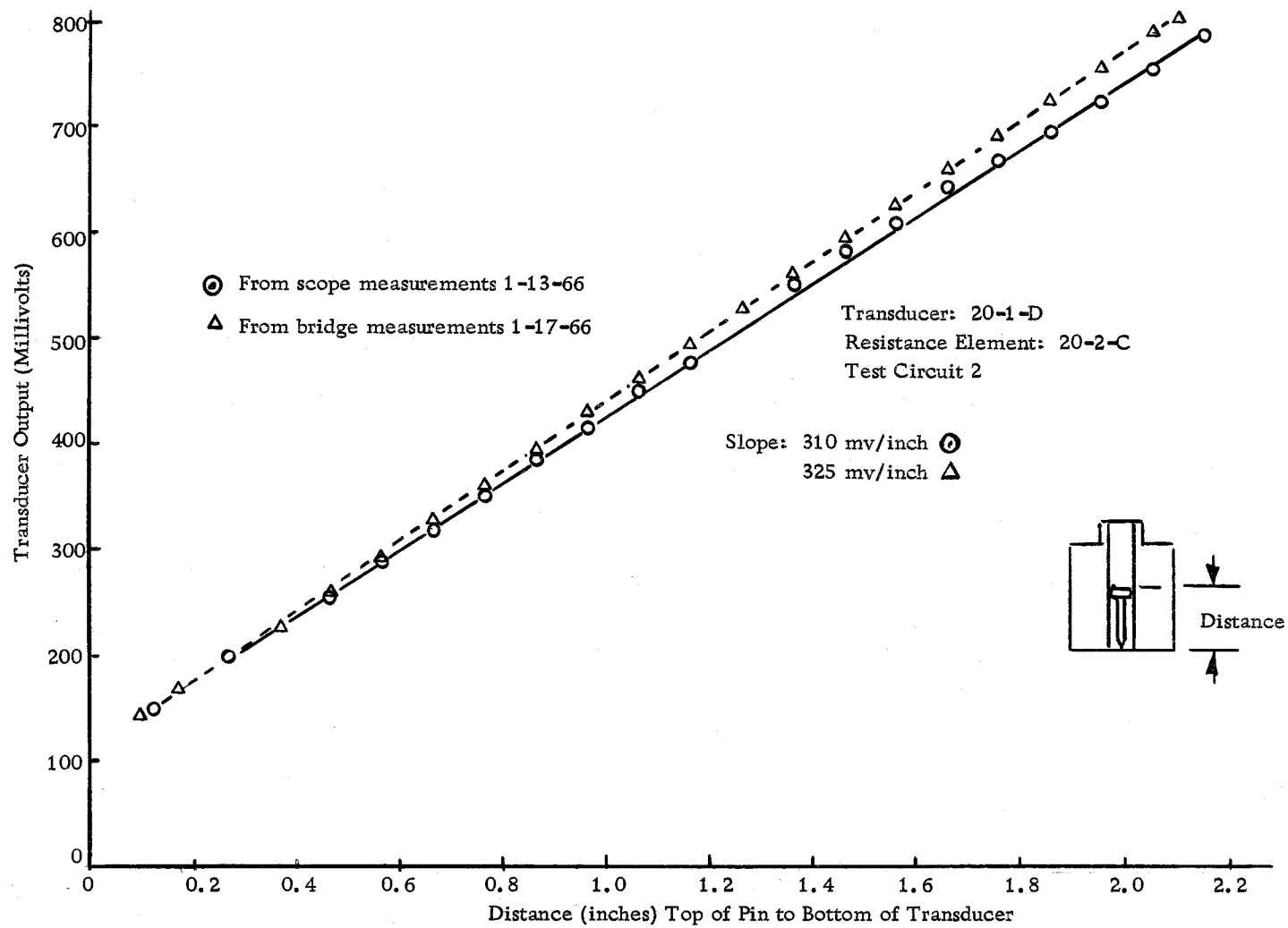


Figure 6. Transducer 20-1-D output vs. pin position

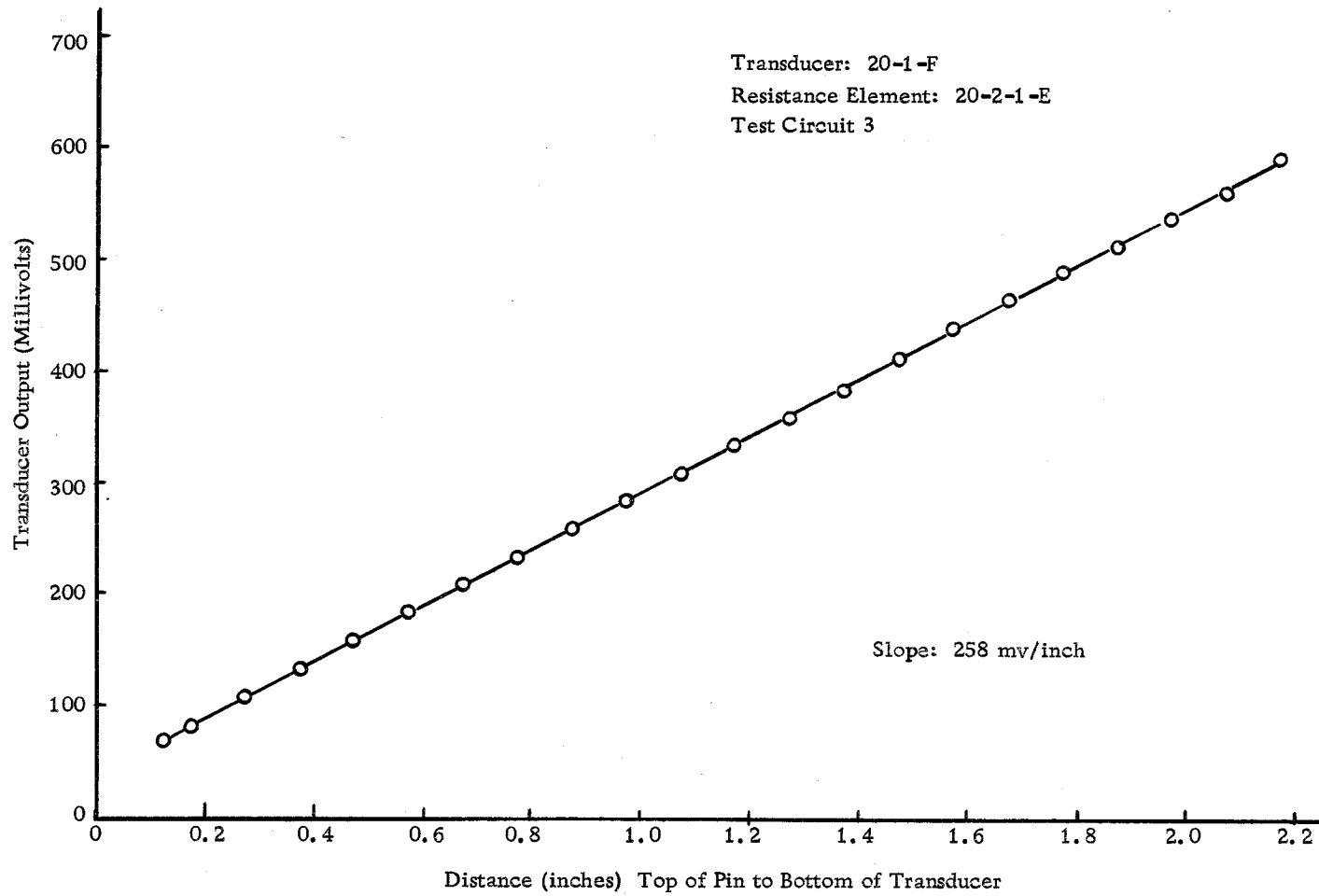


Figure 7. Transducer 20-1-F output vs. pin position

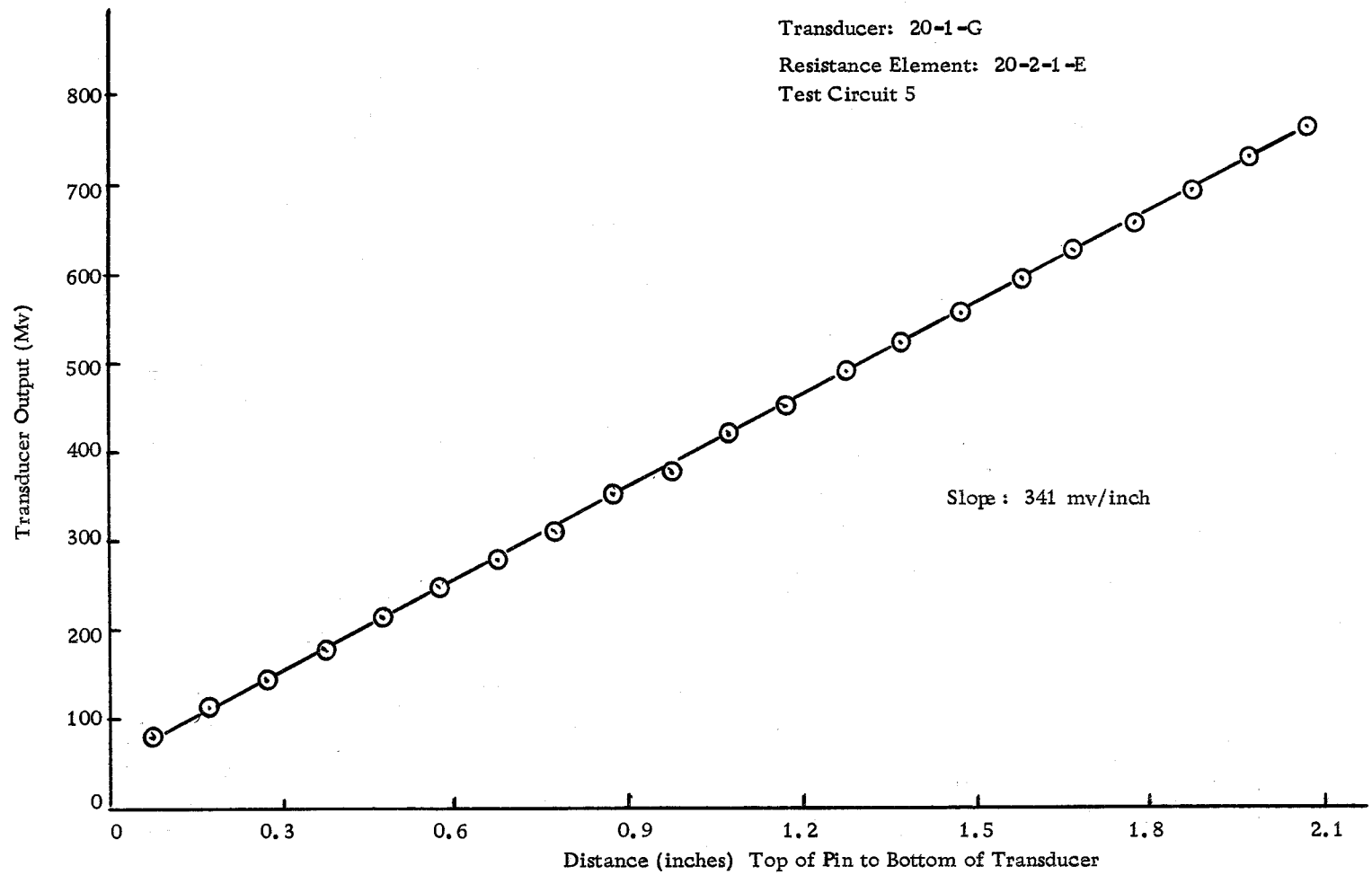


Figure 8. Transducer 20-1-G output vs. pin position

#### IV. EXPERIMENTAL RESULTS

Six experiments were conducted to reveal the characteristics of the measuring system.

Test A consisted of four shots using a wire resistance element and a separate wiper attached to each drivepin. The results indicated that the mechanical strength of the wiper was insufficient. However, a shot with a modified wiper did yield drivepin position versus time information indicating the measuring system had promise.

Test B consisted of 12 shots using a resiliently mounted 0.003 inch Nichrome resistance ribbon and a 0.003 inch stainless steel collector. The wiper of Test A was removed, and the head of a standard drivepin contacted the resistance element and served as a wiper. Although 12 shots were fired, only four were captured on film. These photographs yielded good position versus time information except for the data lost during the time required for internal triggering. This test was terminated when the adhesive bond broke between the elastometer and the resistance element.

Tests C and D used a resiliently mounted 0.007 inch Tophet C resistance element and a 0.003 inch stainless steel collector and a new external triggering circuit. Test C (ten shots) showed that a complete plot of the penetration position versus time could be obtained, but there were periods of lost wiper contact. Test D (three



shots) incorporated an increased contact pressure, but had to be terminated when the collector failed.

Tests E and F consisted of 11 shots using the same resistance element as Tests C and D, and a new 0.010 inch spring steel collector. The aim of these tests was to determine if the tool motion or bounce, observed in previous tests, occurred during the time of drivepin penetration. This motion of the tool adds to the output of the transducer and shows the position of the drivepin with respect to the tool and not the absolute penetration distance. These tests showed that some tool motion does occur during the time of pin penetration. The tests were terminated when the resistance element failed.

The specific details and data are shown in the following pages of this section.

#### Test A

Transducer. Linear potentiometer (0.013 inch diameter Manganin resistance wire mounted on phenolic) recessed in barrel with special wiper fixed to each drivepin. See Transducer 20-1-C, Figure 9.

Circuit. Constant current with internal trigger. See Test Circuit 1, Figure 12.

Drivepin. Two inches long with special wiper attached. See

Wiper and Pin assembly, Figure 14.

Base Material. 1/4 inch cold rolled steel on a 12 x 12 timber.

Test Details. See "Test Description A," Appendix III.

Data. Figure 15 shows the first useable output.

Discussion. This system utilized a modified drivepin consisting of a full hard beryllium-copper wiper soldered under the head of a standard drivepin. This wiper was intended to eliminate damage to the resistance element caused by any lateral motion of the drivepin. However, the acceleration due to the impact of the piston caused the wiper arms to fold over the drivepin head, thus losing contact with the resistance element. This type of response had been anticipated, assuming a wiper of the proper stiffness could be found after preliminary tests.

The first three shots yielded no velocity information due to the loss of wiper contact. The first bit of velocity data was obtained in Test A-1. Before this test, a pin-wiper assembly was modified by hand as shown in the insert of Figure 14. The piston forced the arms down on the head of the drivepin extending the knees of the wiper against the resistance element. Figure 15 shows a semi-continuous plot of transducer output voltage versus time showing that a useful signal can be obtained by this method.

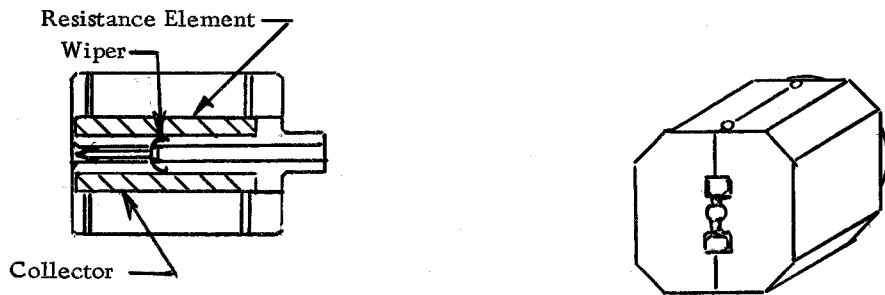


Figure 9. Transducer 20-1-C\*

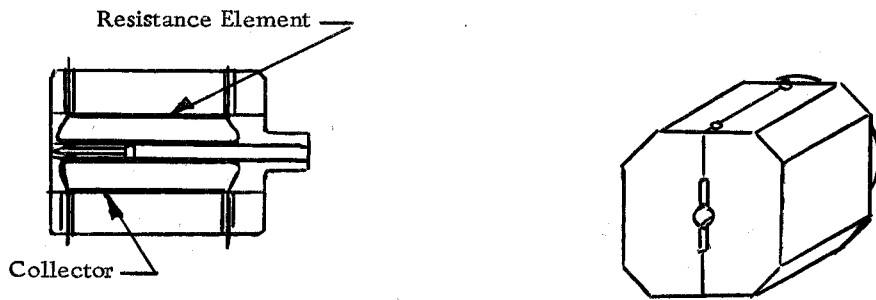


Figure 10. Transducer 20-1-D\* and 20-1-F\*

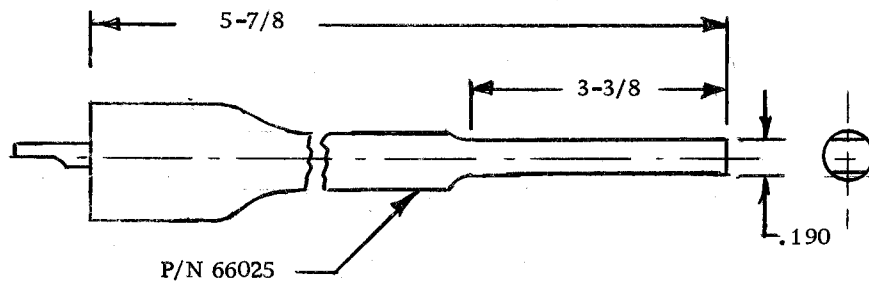


Figure 11. Piston 20-4-3-A

\* Detail dimensions shown in Transducer 20-1-G

The trigger signal for starting the oscilloscope sweep was obtained from the initial change in the transducer output or the initial change in the oscilloscope input. The oscilloscope was set so that the sweep would start as soon as the signal reached a predetermined level (approximately  $1/2$  division below the initial dc level). However, as seen from Figure 15, the sweep must have triggered accidentally, since the first position versus time information starts at the original drivepin ordinate, but is approximately 0.2 milliseconds after the start of the sweep. Note the two dots on the left margin. The top point corresponds to the transducer output with the drivepin in its initial position,  $y_1$ , and the lower point corresponds to the pin's final position,  $y_2$ .

Since the output voltage is assumed to be proportional to the displacement of the head of the drivepin with respect to the barrel of the tool as previously mentioned, this plot will be referred to as the displacement versus time plot.

Since Test A was the first exploratory experiment, the manufacturing tolerance of the Manganin resistance wire was considered to yield sufficient linearity with respect to distance along the wire. However, prior to later tests the output voltage was determined for every 0.100 inch of drivepin travel and the data plotted. See Figures 6, 7, and 8.

After seeing the extent of the wiper damage, it was decided to

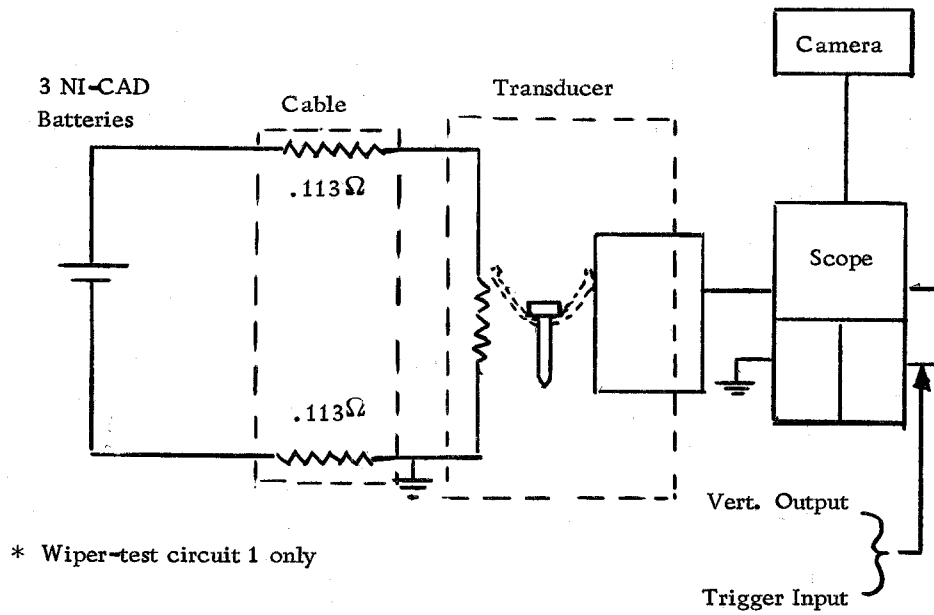
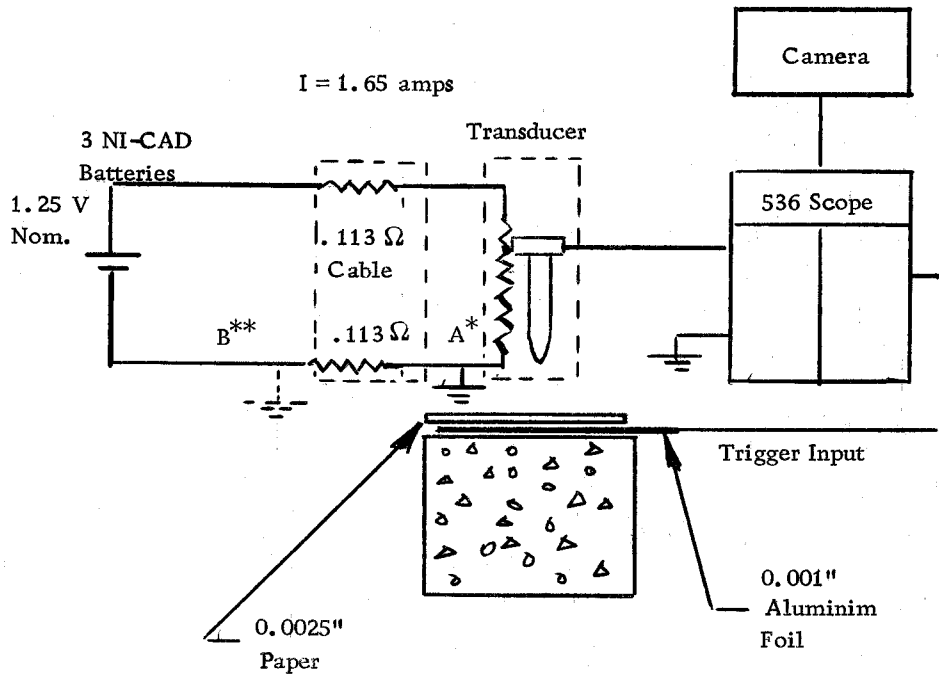


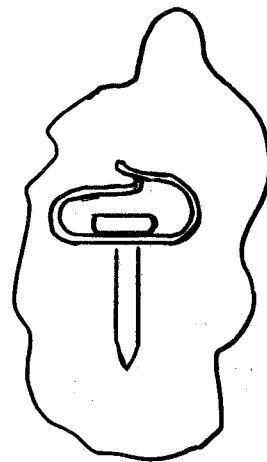
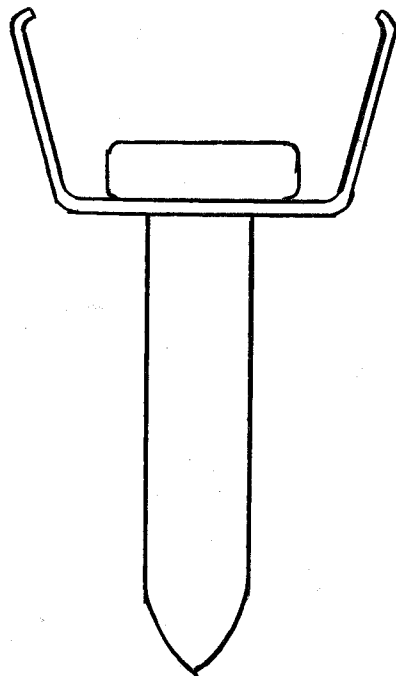
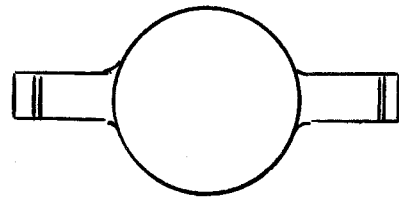
Figure 12. Test circuits 2 and 2



\* Ground for test circuit 3

\*\* Ground for test circuit 4

Figure 13. Test circuits 3 and 4

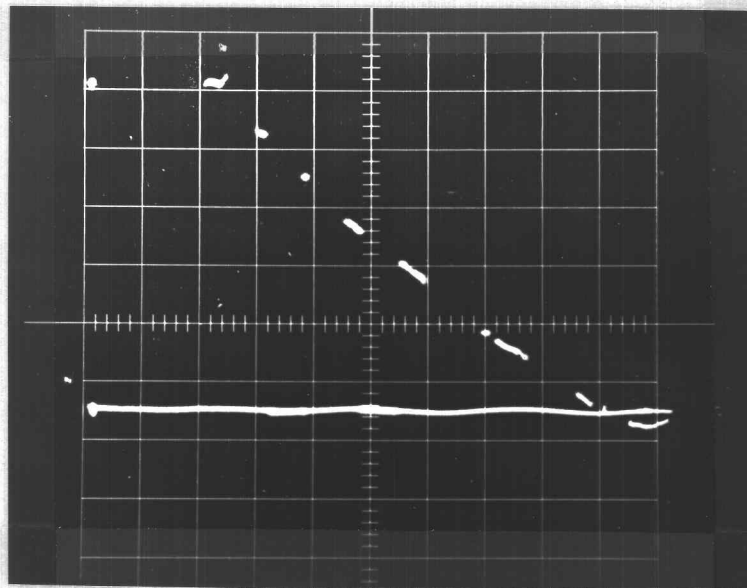


Modified Wiper  
for Test A-1

Figure 14. Wiper and pin assembly

eliminate the wiper rather than change its spring constant. This approach assumes more risk of damaging the resistance element, but has the advantages of not requiring expensive modification of drivepins and not changing the performance of the drivepin by the effect of the wiper. The advantage of using drivepins becomes more attractive as greater numbers of firings are required.

Test B is the first test of the transducer without a wiper attached to the drivepin.



Vert. Sens. = 0.25 inch/div    Hor. Sens. = 0.1 ms/div    Calib. Vert. Sens. = -- inch/div

Figure 15. Transducer output, Test A-1

Test B

Transducer. Linear potentiometer (0.003 inch x 0.062 inch Nichrome resistance ribbon) resiliently mounted in barrel with piston guide. See Transducer 20-1-D, Figure 10.

Circuit. Constant current with internal trigger. See Test Circuit 2, Figure 12.

Drivepin. Standard 1-1/4 inches and 1-1/2 inches with plastic guide. (P/N 47848 and P/N 47849.) See Figure 2.

Piston. Special relieved piston. See Piston 20-4-3-A, Figure 11.

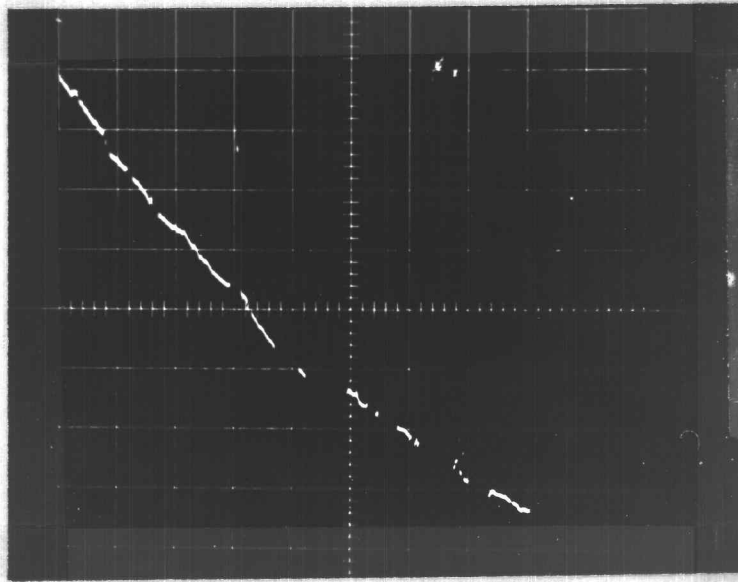
Base Material. 1/4 inch cold rolled steel on a 12 x 12 timber.

Test Details. See "Test Description B," Appendix IV.

Data. Figure 16 shows the initial position of the drivepin as the dot in the upper left corner. The lack of signal between this initial point is the initial deflection of the drivepin that is necessary before the internal trigger starts the sweep. That is, the oscilloscope was set to trigger when the signal went downward through  $y = +4$ .

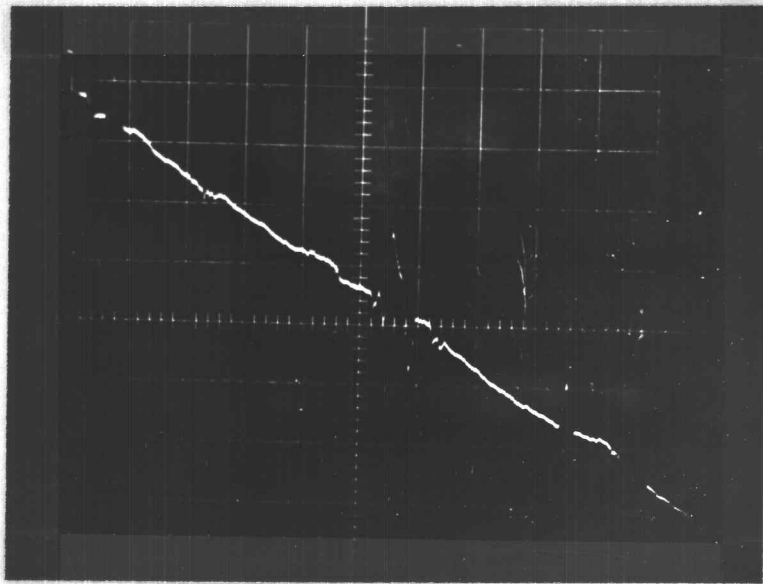
Figure 17 is similar to Figure 16 except the horizontal sensitivity was increased from 0.1 ms/div to 0.05 ms/div. The lower position of the initial point is probably due to the drift of the circuit. This drift is caused by temperature effects of self-heating and of the





Vert. Sens. = -- inch/div    Hor. Sens. = 0.1 ms/div    Calib. Vert. Sens. = 0.154 inch/div

Figure 16. Transducer output, Test B-1



Vert. Sens. = -- inch/div    Hor. Sens. = 0.05 ms/div    Calib. Vert. Sens. = 0.15 inch/div

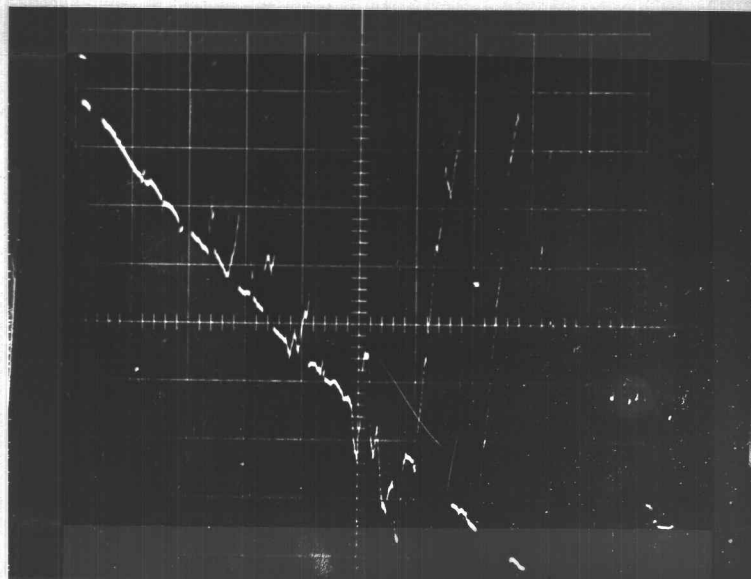
Figure 17. Transducer output, Test B-2

drop in battery output under load. It also may have been a shift of the vertical position of the oscilloscope or the drivepin. The trace indicates an almost constant velocity for the 0.5 ms shown. Remember that time from the initial movement of the drivepin to the start of the sweep is not known.

Figure 18 has the same vertical and horizontal sensitivity as Figure 16 and shows essentially the same information.

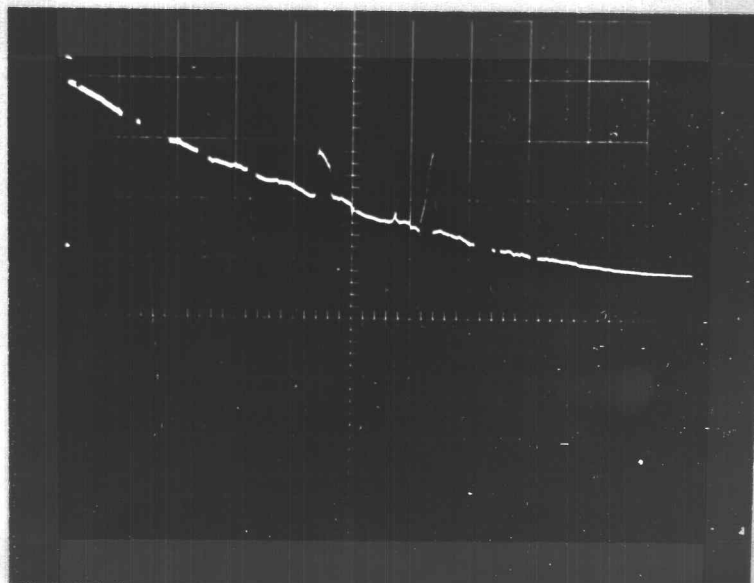
Figure 19 has the first appearance of being a perfect shot with the exception of the few gaps in the trace. The initial position is shown, the velocity is shown continuously until it reaches zero (the slope of the trace becomes zero), and the final position of the drivepin is shown (lower dot on the left margin). However, a closer look at the ordinate of the final position of the trace and the final dot on the left margin show that the trace indicated that the pin penetrated to  $y = 0.8$ , but the final position of the drivepin was  $y = 1.2$ . This could be due to the tool bounce which will be considered later, or, as further inspection of the transducer indicated, due to the damaged resistance element extending into the barrel and shorting to the piston. Note also the change in vertical sensitivity from 50 mv/div as in the previous firings to 100 mv/div.

Discussion. Test B was the first test of the transducer using the head of the drivepin as a wiper. This change made it necessary to move the resistance element and the collector (for reasons of



Vert. Sens. = -- inch/div    Hor. Sens. = 0.1 ms/dv    Calib. Vert. Sens. = 0.15 inch/div

Figure 18. Transducer output, Test B-3



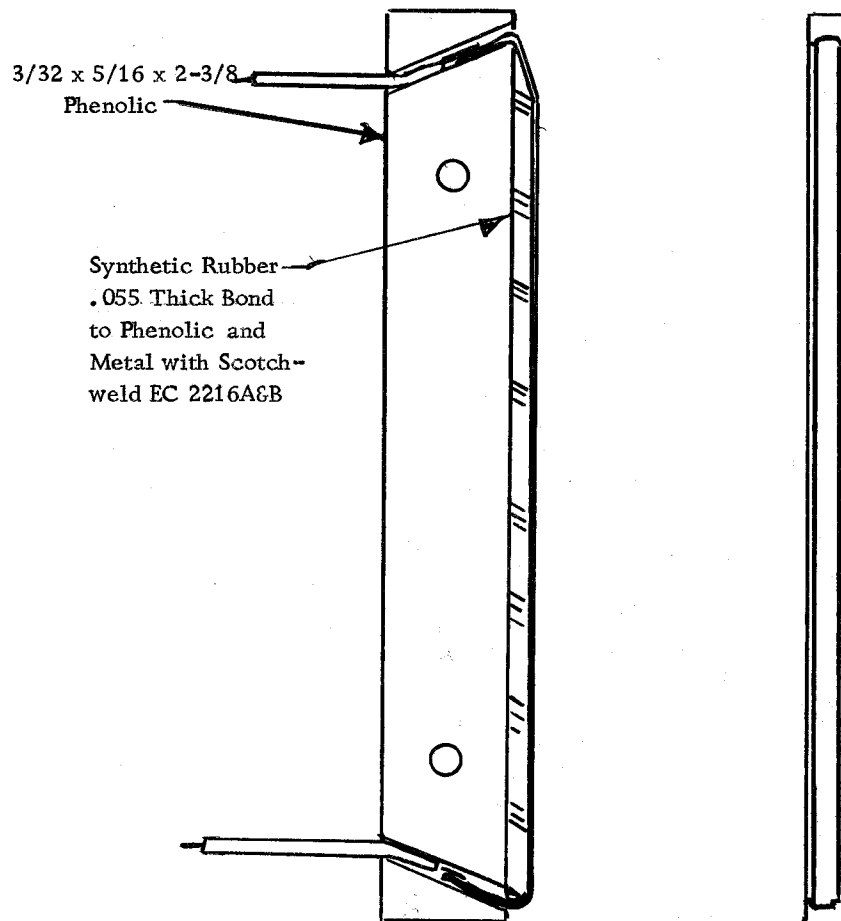
Vert. Sens. = 0.27 inch/div    Hor. Sens. = 0.1 ms/dv    Caib. Vert. Sens. = 0.31 inch/div

Figure 19. Transducer output, Test B-4

symmetry) into the barrel so that the head could bear on them. It was also considered necessary to mount both the resistance element and the collector on a resilient substrate to provide consistent contact force because drivepin head diameters vary, and to minimize damage to both elements during any lateral drivepin motion. This was done by bonding the resistance element and the collector to strips of rubber and bonding the rubber to phenolic. See Resistance elements and collectors 20-2, Figure 20.

The placement of the resistance element and collector in the barrel made it necessary to find a method of keeping the piston, which has the same diameter as the head of the drivepin, from making electrical contact with the resistance element. This was done by grinding flats on opposite sides of the piston (see Piston 20-4-3-A, Figure 11) and providing a piston guide to keep the flats opposite the resistance element. Grinding the flats on the piston changed its mass such that it does not represent the actual operating conditions. However, the reduction in mass may be considered insignificant. The mass of a standard piston (P/N 66025) is 51.35 grams and the mass of the ground piston is 48.50 grams or 94.5 percent of its normal value. This fact becomes less important when it is realized that there are four lengths of standard pistons which are used with this tool.

In all the discussions of the photographs, consider the center



## Resistance Element:

20-2-B

.013 Dia. Manganin Wire  
(No rubber)

20-2-1-C

.003 x .062 x 2.63 NI-chrome

20-2-1-E &amp; 20-2-F

.007 x .042 x 2.63 Tophet C

## Collector:

20-2-B

.031 Dia. Music Wire  
(No rubber)

20-2-2-C &amp; 20-2-2-E

.003 x .093 x 2.63  
Stainless Steel

Figure 20. Resistance elements and collectors 20-2

of the graticule (grid) as the origin and the  $x$  divisions positive to the right and the  $y$  divisions positive upward.

Since the initial deflection of the drivepin must occur before the sweep or time base starts, the only interpretation of the trace from  $y = y_1$  to the start of the sweep is that the drivepin travelled that many divisions (inches) in an undetermined time. Once the sweep starts, though, the drivepin travel is recorded as a function of time. The slope of this plot is proportional to the pin velocity. The gaps in the trace are due to interruption of contact of the head of the pin with the resistance element and/or the collector or barrel. The waviness of the trace may be due to active or passive noise or to change of the point of contact of the drivepin head on the resistance element. The head of the drivepin is approximately 0.075 inch thick, but the flattest portion is the middle 0.050 inch. If the point of contact changed from the top to the bottom of the drivepin head, the output voltage should change 28 mv which would be more than  $1/2$  of a division. Still, some rocking of smaller magnitude may take place. The waviness may also be a true picture of the actual drivepin travel.

The loss of the time base during the first travel of the drivepin indicated that a separate trigger mechanism should be found so that the sweep will start at the same time as the motion of the drivepin. This was accomplished by placing a small piece of aluminum

foil 0.001 inch thick on the surface of the workpiece and separating the foil from the tool with a piece of paper 0.0025 inch thick. Since the drivepin head contacts the resistance element, the initial voltage will be transferred to the foil as soon as the point of the drivepin pierces the paper. This voltage can be used as an external trigger for the sweep.

The damage of the resistance element referred to earlier consisted of the 0.003 inch Nichrome breaking its bond with the rubber and forming a bump or wave which projected into the barrel. The piston touched the bump and caused the output to appear as if a drivepin was at that location.

Test C incorporated a new resistance element and the new trigger circuit. The new resistance element is approximately twice as thick as the one for Test B.

### Test C

Transducer. Linear potentiometer (0.007 inch x 0.047 inch Tophet C resistance ribbon) resiliently mounted in barrel with piston guide. See Transducer 20-1-F, Figure 10.

Circuit. Constant current with external foil trigger. See Test Circuit 3, Figure 13.

Drivepin. Standard 1-1/2 inches with plastic guide (P/N 47849). See Figure 2. (All drivepins for this and subsequent tests had head

diameters ranging from 0.2365 inch to 0.2369 inch.)

Base Material. Concrete slab, 3000 psi.

Test Details. See "Test Description C," Appendix V.

Data. Figure 21 shows an interrupted plot of the penetration velocity. The initial loss of contact occurs at almost the same time and place (allowing for the shift in initial position) as it did in Figure 23. Inspection of the resistance element after Test C revealed a valley 0.1 inch long at approximately 0.3 inch travel for a 1-1/2 inch drivepin. This photo also shows final position  $y_2$  which corresponds to the position of the trace as it travels off the right margin.

Figure 22 is a "perfect" shot except for the one moment of lost signal at  $x = -2.5$ . The sweep started from an unknown cause approximately 0.1 millisecond before the drivepin started to move and the pin came to rest before the trace went off the right margin. This, then, shows a continuous picture of the drivepin position before, during, and after penetration. Note also that at this sweep speed, the velocity appears to jump from zero to a finite velocity.

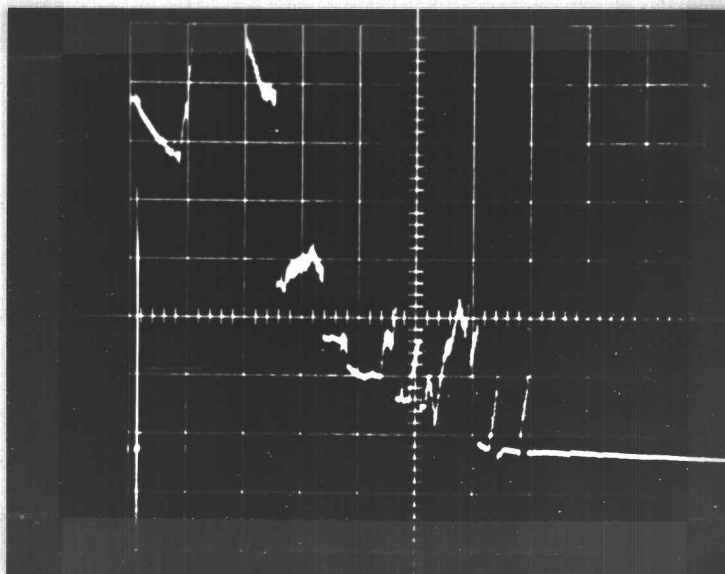
Figure 23 has more points of discontinuity than Figure 22 but, assuming the good data represent a continuous function, it is still a good shot. Note that the initial velocity appears to be instantaneously finite.

Figure 24 is a good shot with a minimum amount of missing data. Note the apparent segments of zero velocity at  $x=0$  and  $x=1$ .



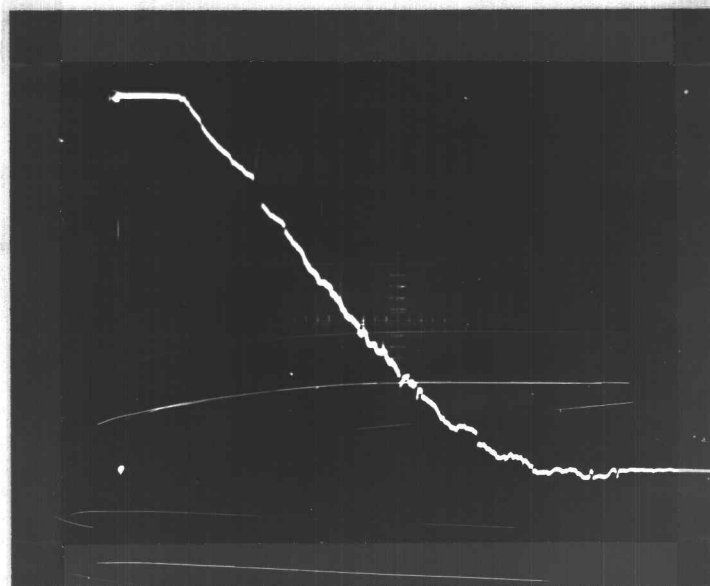
Figure 25 shows the tool and transducer, the concrete into which the pins were fired, the pins, and the foil and paper trigger. Note spall or splattered concrete. The two by fours and other pins in the background were not part of this test.

Discussion. Test C showed that the foil-paper trigger does allow the recording of the velocity information from the first motion of the drivepin, that the information can be continuous, and that the mechanical strength of the transducer, both resistance element and collector was marginal. Inspection of the transducer after this test revealed that the .003 inch x .093 inch stainless steel collector (20-E-2-E) had become separated from the rubber base. However, this did not render the transducer inoperative since the whole barrel serves the same electrical function. The resistance element remained bonded to the rubber (ten shots thus far) but it had formed a permanent valley approximately 0.100 inch long, as noted in Figure 21. It was very difficult to adjust the triggering level since the magnitude of the trigger voltage was very nearly the minimum voltage which can start the sweep in the Type "T" plug-in. Noting that the signal voltage and trigger voltage were measured with respect to the lower end of the resistance element, point A, Test Circuit 3, it is obvious that some increase in the magnitude of the trigger voltage can be obtained by measuring the voltages with respect to point B. For this test the increase in trigger voltage should be from 400 mv



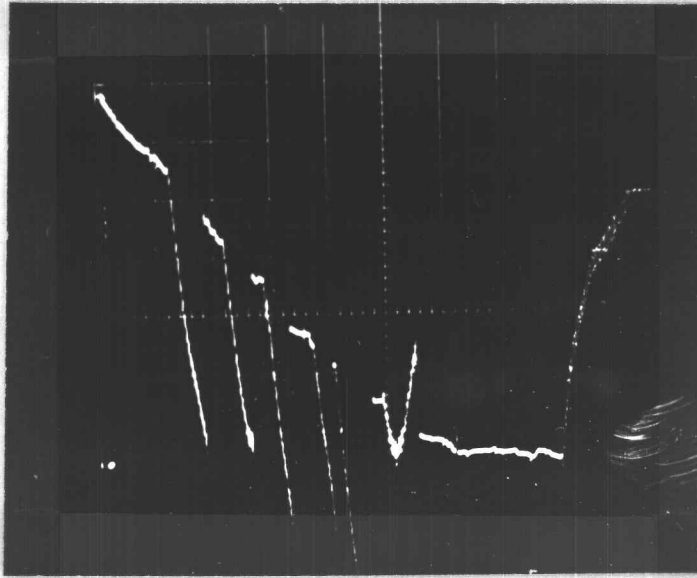
Vert. Sens. = 0.19 inch/div    Hor. Sens. = 0.1 ms/div    Calib. Vert. Sens. = 0.194 inch/div

Figure 21. Transducer output, Test C-1



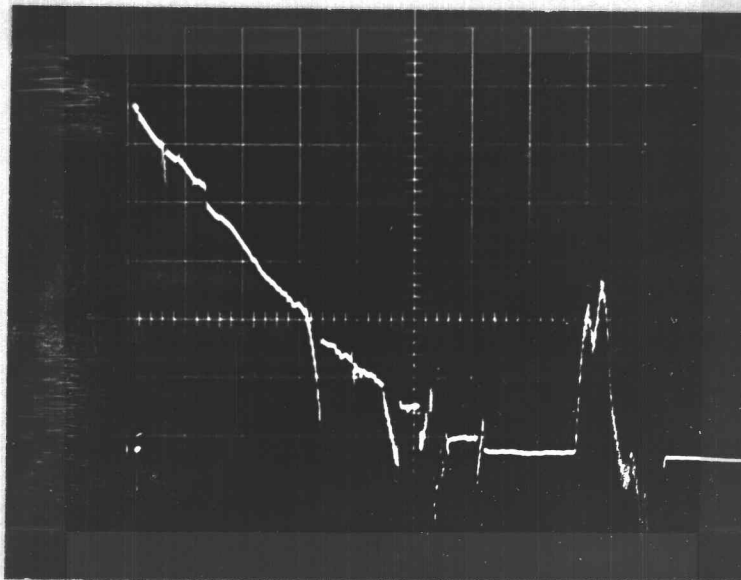
Vert. Sens. = 0.20 inch/div    Hor. Sens. = 0.1 ms/div    Calib. Vert. Sens. = 0.194 inch/div

Figure 22. Transducer output, Test C-2



Vert. Sens. = 0.19 inch/div   Hor. Sens. = 0.1 ms/div   Calib. Vert. Sens. = 0.194 inch/div

Figure 23. Transducer output, Test C-3



Vert. Sens. = 0.20 inch/div   Hor. Sens. = 0.1 ms/div   Calib. Vert. Sens. = 0.194 inch/div

Figure 24. Transducer output, Test C-4

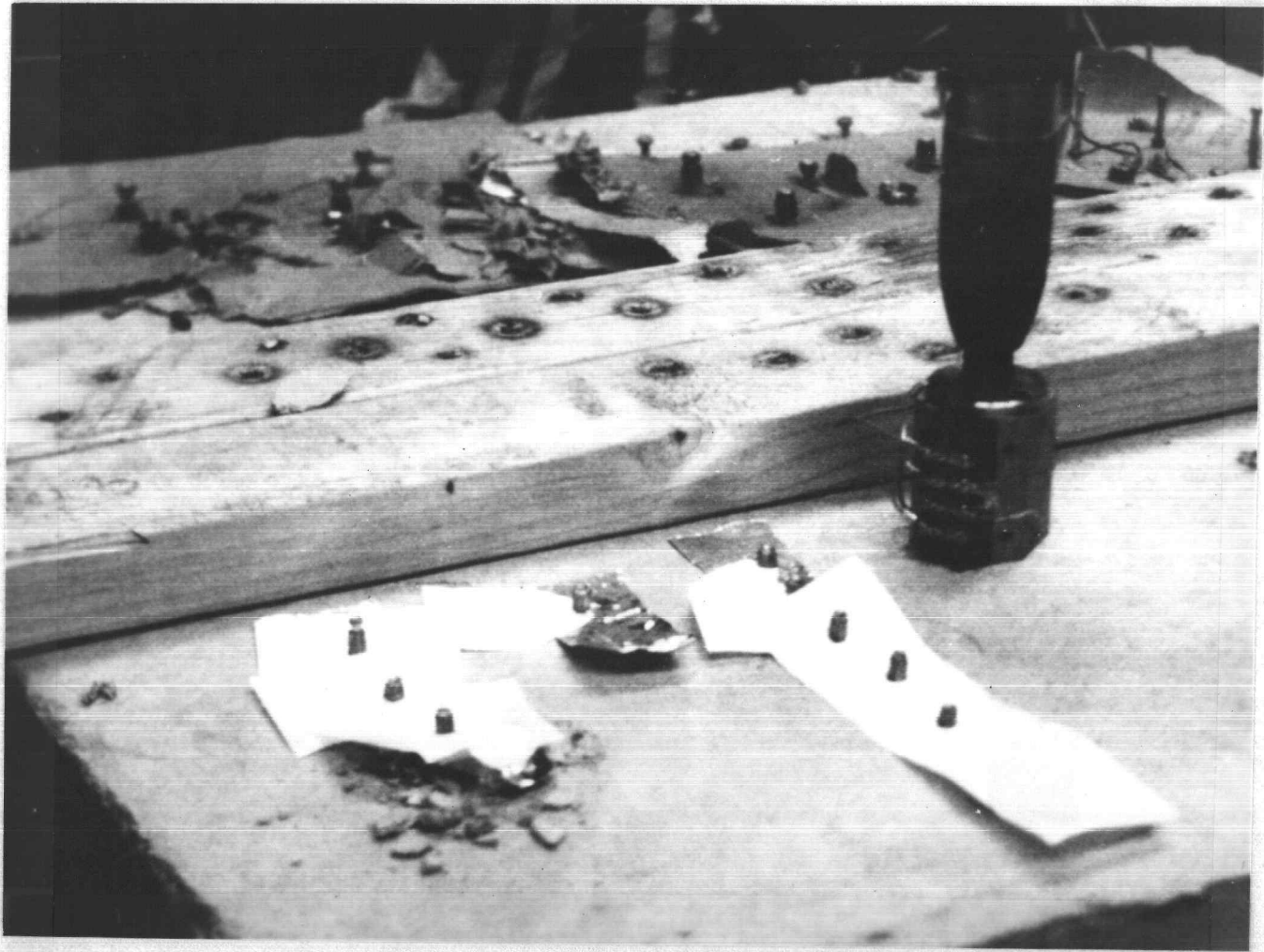


Figure 25. Test C

to 600 mv. The minimum trigger voltage requirement of the oscilloscope is 200 mv.

The dynamic friction force on each drivepin (measured by forcing a drivepin into the transducer on scale) was of the order of three to five ounces. This was recorded to show the magnitude of the forces of the measuring system which could change the performance or action of the drivepin.

Since there was difficulty in obtaining sufficient trigger voltage and maintaining contact with the resistance element, Test D was planned to evaluate the effect of increasing the trigger voltage and the contact pressure of the drivepin. The trigger voltage was increased by considering the system ground at point B, Test Circuit 3.

#### Test D

Transducer. Linear potentiometer (0.007 inch x 0.047 inch Tophet C resistance ribbon), resiliently mounted in the barrel with a piston guide. See Transducer 20-1-F, Figure 10. This is the same transducer used in Test C, with minor damage evident in the collector.

Circuit. Constant current with external foil trigger. See Test Circuit 4, Figure 13.

Drivepin. Standard 1-1/2 inches with plastic guide (P/N 47849). See Figure 2.

Base Material. Concrete slab, 3000 psi.

Test Details. See "Test Description D" Appendix VI.

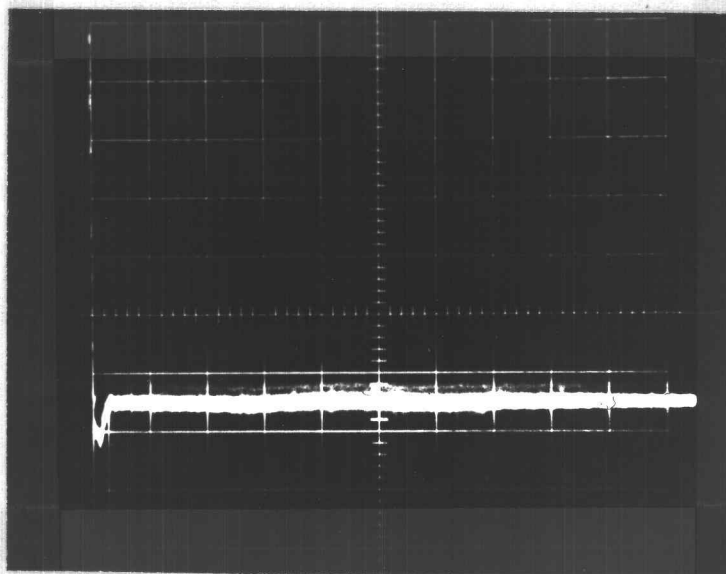
Data. Figure 26 was taken at a much slower sweep than any previously taken--actually one five-hundredth of the usual sweep rate. This, then, shows an apparent jump from initial position to final position in zero time, virtually eliminating the determination of the time of penetration. The dip from the final position and back is significant. More will be said of this in the discussion.

Figure 27 shows  $y_1$  and  $y_2$  plus the initial portion of the velocity. Note that the trace is free of noise or random signals. The drivepin bent as it entered the concrete accounting for the loss of signal.

Figure 28 shows the tool, concrete, and the test equipment. The apparatus under the oscilloscope is the batteries for the transducer.

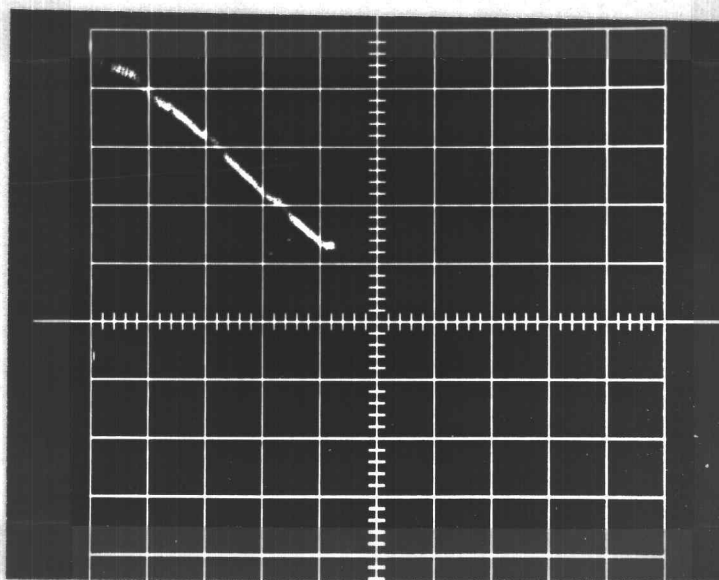
Figure 29 shows the broken 0.003 inch x 0.094 inch stainless steel collector.

Discussion. This test was intended to evaluate the effect of increasing the contact pressure on the drivepin. Only one photo was obtained showing the velocity information because the sweep rate was inadvertently set far too slow. However, if this single photo is considered significant, the drivepin did not lose contact until an abnormal lateral force was encountered--the pin bent in the concrete.



Vert. Sens. = 0.20 inch/div   Hor. Sens. = 50 ms/div   Calib. Vert. Sens. = 0.194 inch/div

Figure 26. Transducer output, Test D-1



Vert. Sens. = 0.19 inch/div   Hor. Sens. = 0.1 ms/div   Calib. Vert. Sens. = 0.194 inch/div

Figure 27. Transducer output, Test D-2

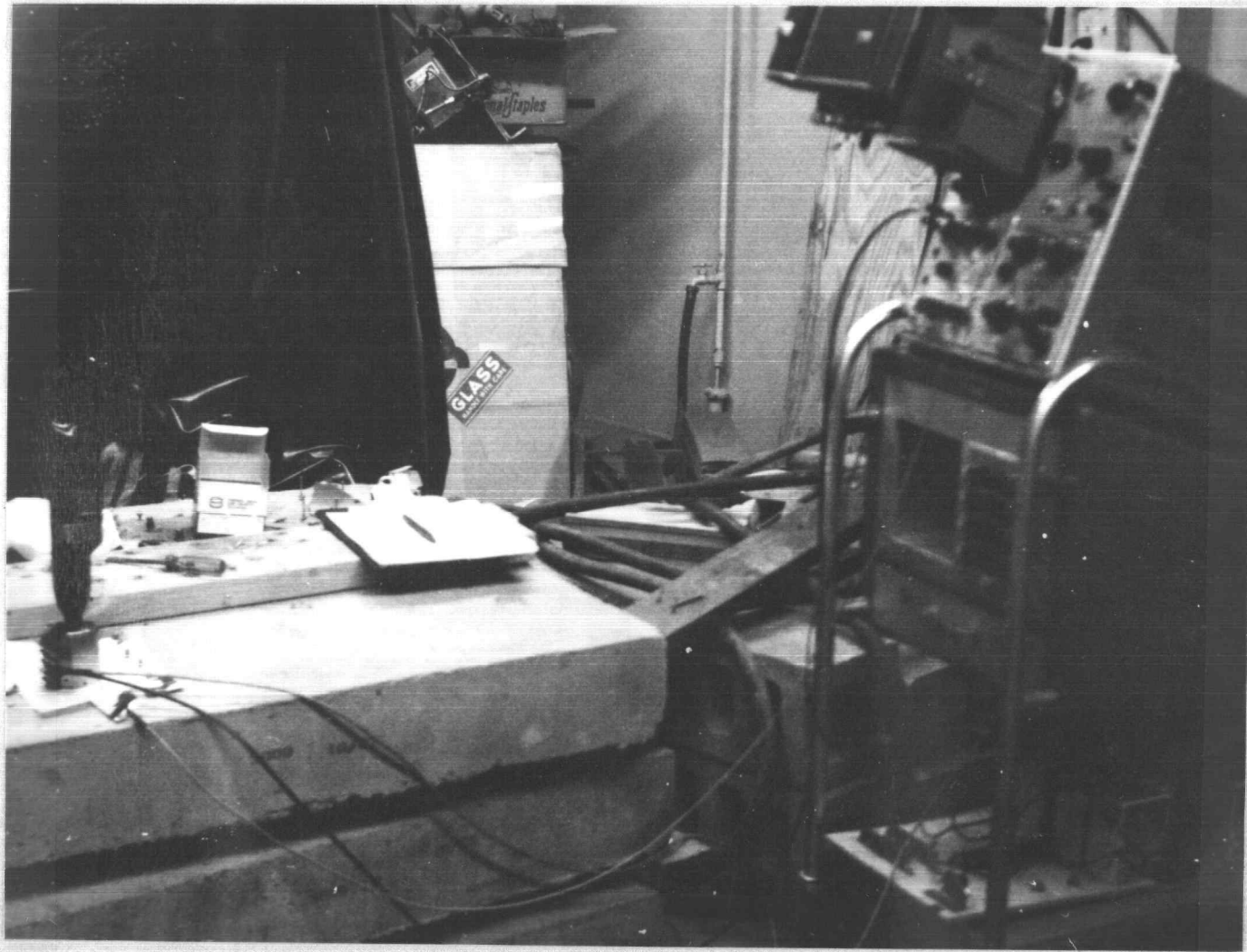


Figure 28. Test D.



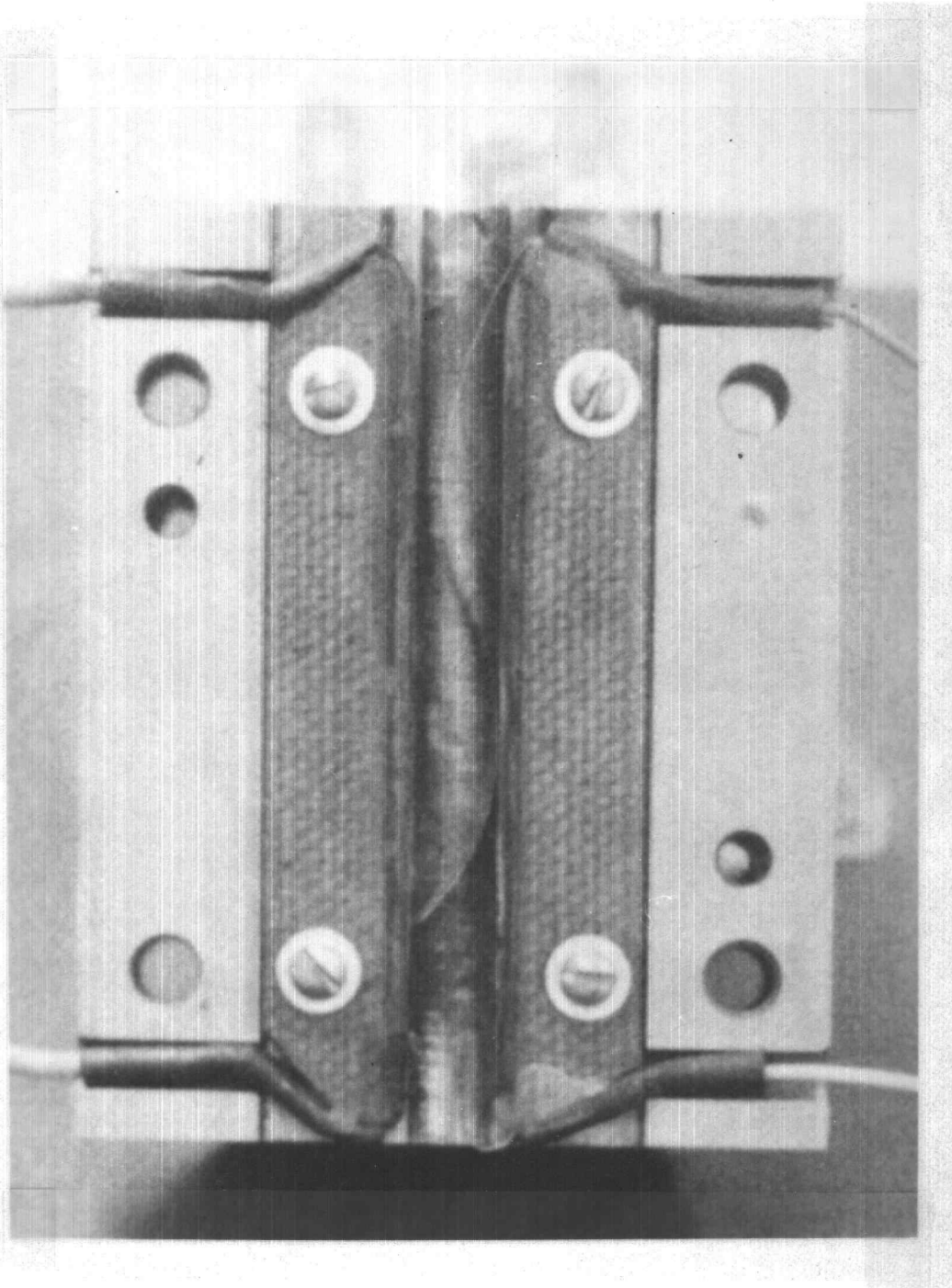


Figure 29. Resistance element and damaged collector 20-2-E

Figure 26 with a 50 millisecond per division sweep shows that the tool did lift off the concrete (bounce) at least after the drivepin had stopped. It does not show, however, whether it bounced during the penetration also. This dip must have been the tool lifting since this is the only way to explain the apparent further penetration of the drivepin into the concrete after it had stopped at  $y_2$ .

The collector failed gradually by first breaking loose from the rubber, then exhibiting a wave action in front of the motion of the drivepin, then finally parting. However, it did last for 25 firings.

The increased contact force was obtained at the expense of friction force on the drivepin and transducer. This dynamic friction force ranged from seven to eleven ounces when the pin was inserted by hand.

This test indicated a need to determine more about the lifting or bounce of the tool. Test E was planned to accomplish this and to test a new collector.

#### Test E

Transducer. Linear potentiometer (0.007 inch x 0.047 Tophet C resistance ribbon) resiliently mounted in the barrel with a piston guide and 0.010 inch thick spring steel collector. See Transducer 20-1-G, Figure 30.



Circuit. Constant current with external foil trigger and foil "bounce" indicator. See Test Circuit 5, Figure 31.

Drivepin. Standard 1-1/2 inches with plastic guide (P/N 47849). See Figure 2.

Base Material. Concrete slab, light rock aggregate, 3000 psi.

Test Details. See "Test Description E," Appendix VII.

Data. Figure 32 shows a dual beam trace. The upper beam is the voltage of the drivepin (also the voltage of the barrel); the lower beam is the voltage of the barrel as transmitted to a foil between the barrel and the workpiece. Note that the vertical scale factors are different.

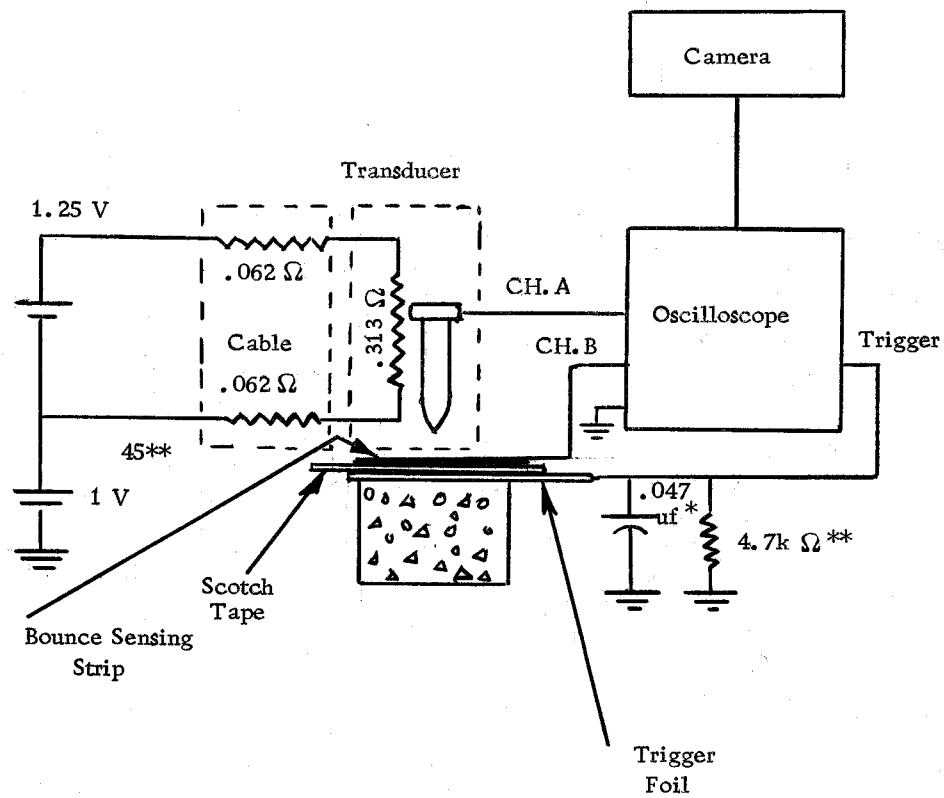
Figure 33 shows quite markedly that the tool did lose contact with the foil at approximately the midpoint of the drivepin travel.

Discussion. The aluminum foil between the tool and the paper tended to follow the tool away from the workpiece and, consequently, a sharp indication of time of bounce was not obtained.

The change in beam intensity of this oscilloscope from before the sweep starts to during the sweep was so intense that the initial and final points  $y_1$  and  $y_2$  were not evident on the film.

The different slopes shown for the same voltages on each beam are due to the different vertical scale factors for each beam.

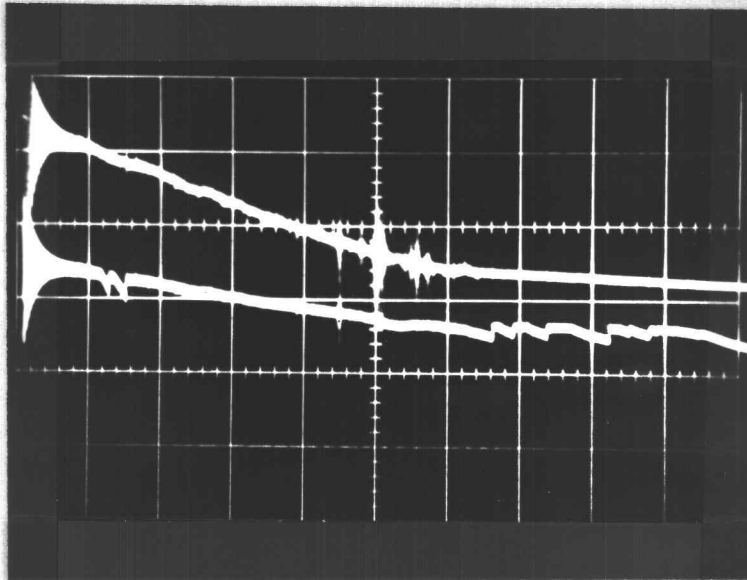
Figure 33 shows a discontinuity of some sort during the drivepin penetration, while Figure 32 seems to indicate by the similarity



\* Test Circuit 5 only

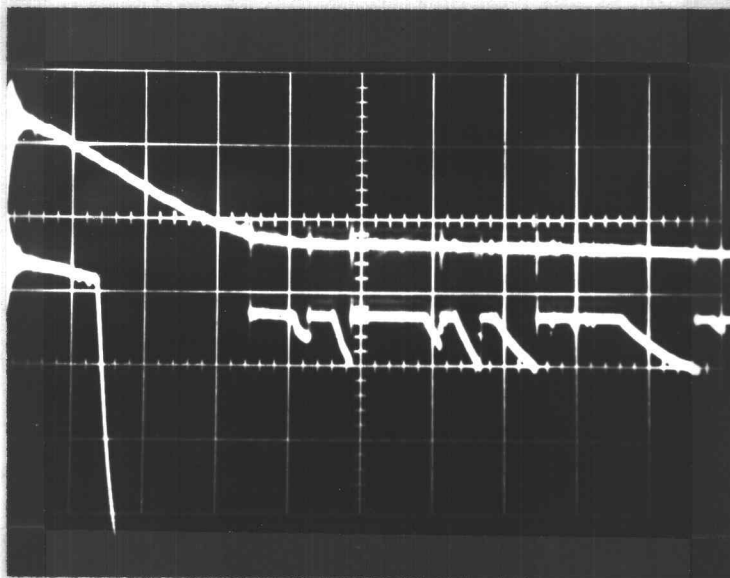
\*\* Test Circuit 6 only

Figure 31. Test circuits 5 and 6



Upper Beam Vertical Scale Factor = 200 mv/div Lower Beam Vertical Scale Factor = 500 mv/div  
Hor. Sens. = 0.1 ms/div

Figure 32. Transducer output, Test E-1



Upper Beam Vertical Scale Factor = 200 mv/div Lower Beam Vertical Scale Factor = 500 mv/div  
Hor. Sens. = 0.2 ms/div

Figure 33. Transducer output, Test E-2

of traces that the tool did not leave the surface of the workpiece. Or, perhaps, the tool bounced and the foil followed the tool, thus maintaining contact.

The force required to insert the pins for this test was approximately 2-1/4 pounds.

This circuit used a new set of cables for the battery circuit (#18 wire).

Inspection of the transducer after Test E showed a slight waviness in the collector and the resistance element had come unglued from the rubber and was projecting into the barrel.

A major problem encountered during this test was the magnitude of 60 cycle noise in the trigger circuit. This was minimized by inserting a 0.047 microfarad capacitor from the trigger foil to the system ground. This allowed the shots to be obtained, but added a small delay of the trigger signal because of the time required to charge the capacitor through essentially zero resistance. The noise before inserting the capacitor was of the same order as the trigger signal. Inspection of the test leads after the test revealed one broken lead (no continuity). This was probably the largest contributor to the noise problem of Test E.

The piston was found to short to the resistance element on occasion after Test E.

In view of the lack of conclusive data from Test E, and the lack

of initial and final drivepin position of the 551 oscilloscope, Test F was planned to use the single trace 536 oscilloscope with a Type CA dual trace plug-in and obtain a more positive indication of tool bounce. An additional battery was also used to increase the trigger voltage to a more acceptable value.

### Test F

Transducer. Linear potentiometer (same as Test E). See Transducer 20-1-G, Figure 30.

Circuit. Constant current with external foil trigger and flat spring stock "bounce" indicator. See Test Circuit 6, Figure 31.

Drivepin. Standard 1-1/2 inches with plastic guide (P/N47849). See Figure 2.

Base Material. Concrete slab, light rock aggregate, 3000 psi.

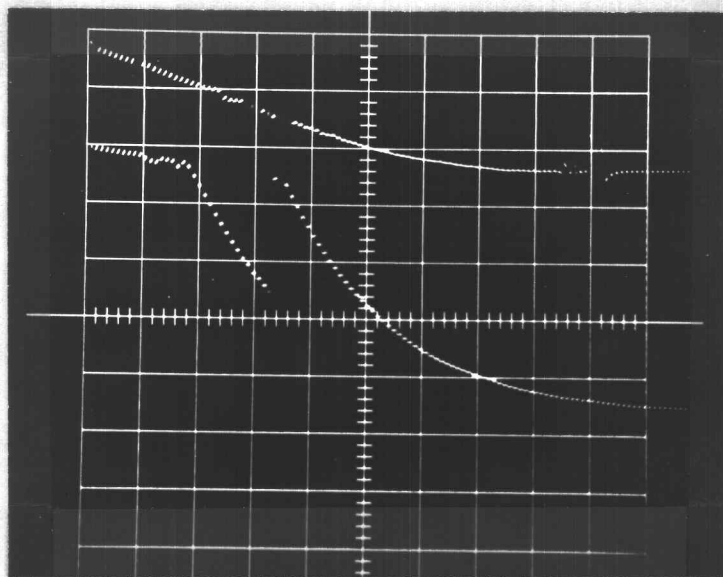
Test Details. See "Test Description F," Appendix VIII.

Data. Figure 34 indicates the tool lost contact with the workpiece for about 0.1 millisecond, returned to the workpiece briefly, then "bounced" again. Note the lack of noise.

Figure 35 shows another definite "bounce" during the drivepin penetration. It also is free of noise.

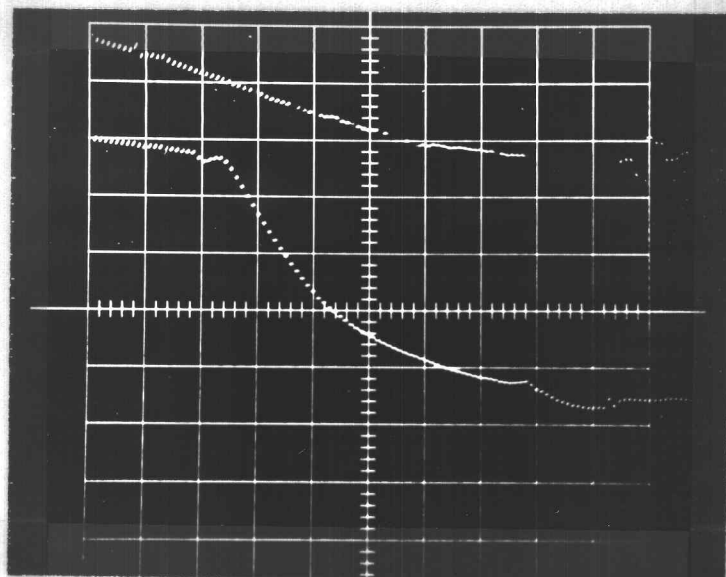
Figure 36 and 37 show the damaged resistance element and collector after Test F.





Upper Beam Vertical Scale Factor = 200 mv/div    Lower Beam Vertical Scale Factor = 500 mv/div  
Hor. Sens. = 0.1 ms/div

Figure 34. Transducer output, Test F-1



Upper Beam Vertical Scale Factor = 200 mv/div    Lower Beam Vertical Scale Factor = 500 mv/div  
Hor. Sens. = 0.1 ms/div

Figure 35. Transducer output, Test F-2

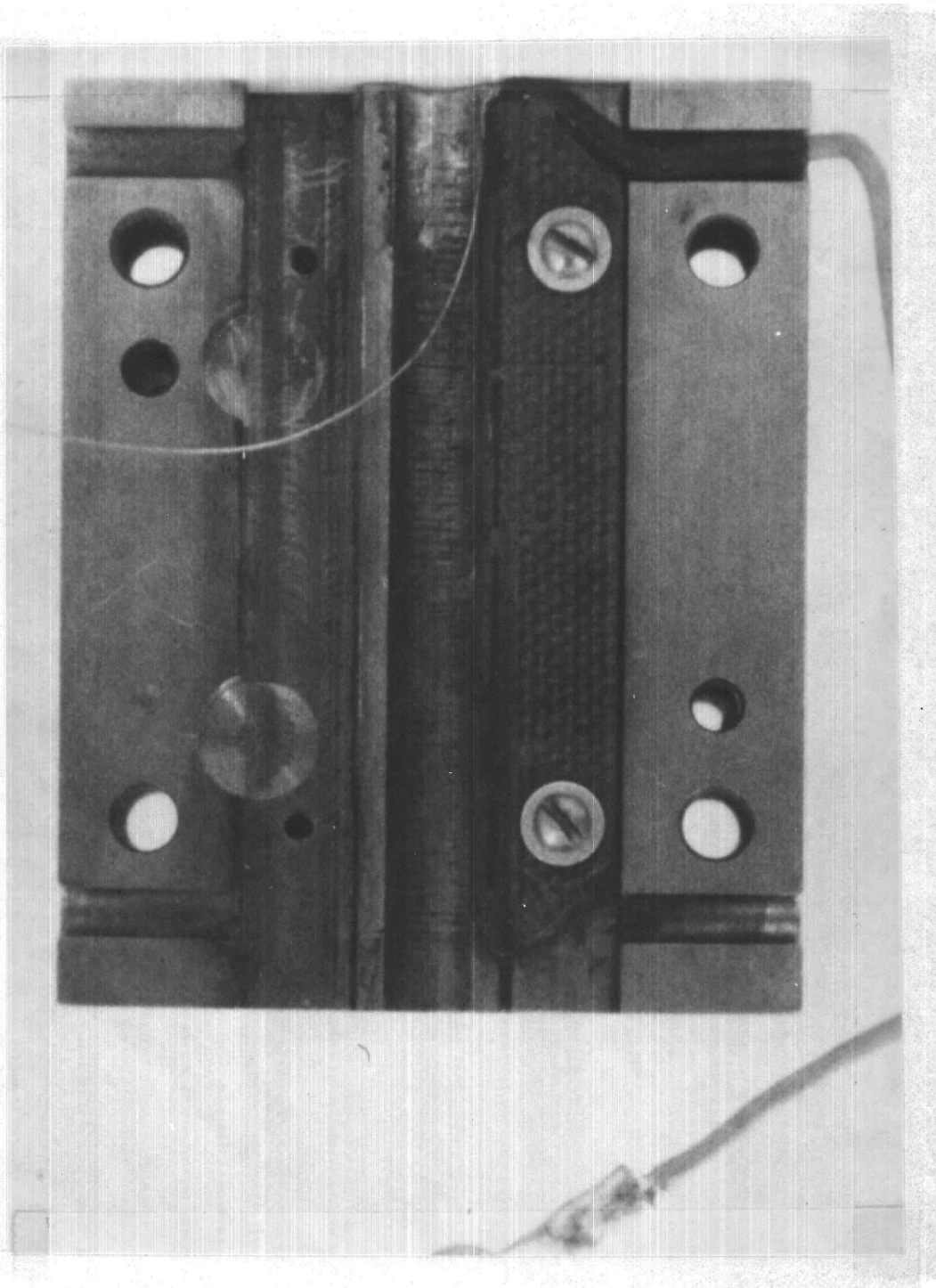


Figure 36. Damaged resistance element 20-2-1-F

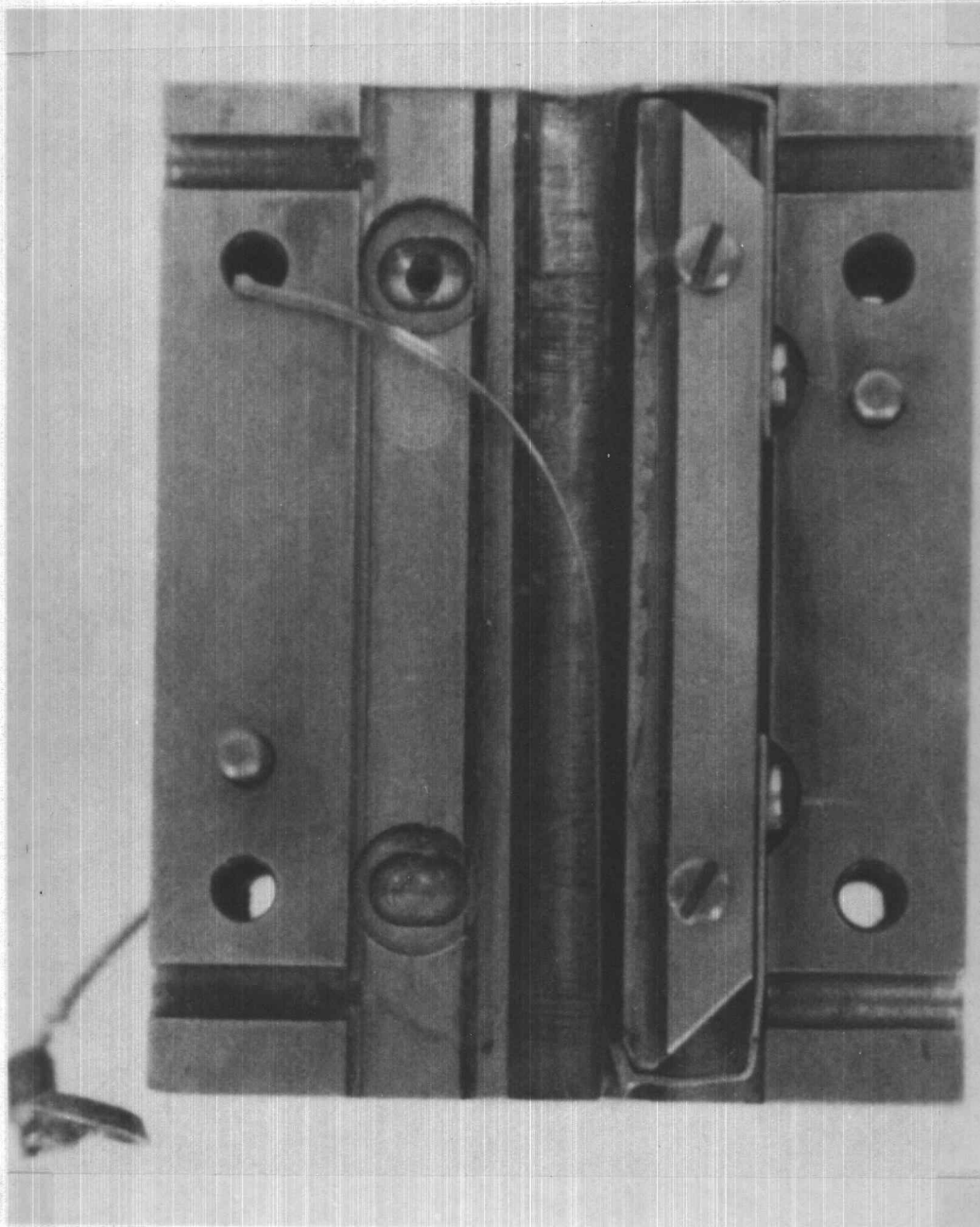


Figure 37. Damaged collector 20-5

Discussion. This test was planned to accomplish two objectives; to obtain a clearer picture of the time of tool bounce, and to reduce the pick-up of noise. Since the resistance element was known to be projecting into the barrel at times, the velocity information was suspect; so the resistance element was only used to supply the needed signal through the drivepin for determining the time of tool bounce.

The clarity of Figures 34 and 35 indicates that noise is no problem with this circuit.

Figures 34 and 35 show that, at least in those two tests, the tool does bounce approximately 0.2 milliseconds after the drivepin motion starts. The exponential decay of the lower beam is the result of the discharge of the capacitor through the input impedance of the oscilloscope. This capacitor is made up of the jump sensing strip, the tape insulator, and the foil trigger. Calculations of the capacitance of a parallel plate capacitor and its time constant yield a time constant of the same order of magnitude as the one shown on the traces.

The circuit of this test had two additions not present in previous tests.

The 1.5 volt battery elevated the whole system above ground so that the trigger voltage was 1.5 volts plus approximately 500 millivolts in the transducer circuit. This increase in voltage helps the trigger circuit, but must not be too high so that a lower oscilloscope

vertical sensitivity would be necessary to keep the signal on scale. The other addition was the  $4.7k\Omega$  resistor from the trigger foil to ground. This reduced the pickup of noise in the trigger circuit to 50 mv at the expense of 0.5 milliamperes additional current from the circuit.

## V. DISCUSSION OF TEST RESULTS

This method of determining the instantaneous position of the drivepin is based on four requirements:

1. That the resistance element is linear with respect to point of contact the drivepin.
2. That the time base calibration of the oscilloscope is reliable.
3. That the transducer circuit is supplied by a constant current source.
4. That the motion of the tool with respect to the workpiece is known.

The first requirement was accomplished by using resistance wire or resistance ribbon which is manufactured to close tolerances of resistance as a function of length. The actual linearity was measured and found to be well within the limits required. Also, the change or deterioration of this linearity caused by pin contact was found to be insignificant after 13 firings. This is shown by comparing the linearity of Figures 7 and 8 which are for the same resistance element but with different battery lead wires, hence different outputs.

The second requirement was assumed to be met by using a recently calibrated Tektronix Type T time base generator for the horizontal sweep.

The third requirement was met by selecting proper circuit components. If this constant current source requirement is met, the output of the potentiometer is a linear function of the drivepin position. Calculations revealed that the dc error would be less than one part per million and the time constant of the oscilloscope would be approximately  $4 \times 10^{-12}$  seconds. Since the pin penetration occurs in approximately  $1 \times 10^{-3}$  seconds, this time constant will allow the circuit to respond to frequencies many orders of magnitude higher than those expected. These calculations are shown in Appendix I. It is interesting to note that the initial calibration and the calibration obtained from each observation check very well. Table 1 shows the method of determining the calibration (vertical sensitivity) for each photograph. The shorting effect of the long contact area of the drivepin on the resistance element was insignificant. The stability of the battery current under load versus time is shown in Figure 38.

The fourth requirement was found to be important since Tests E and F indicated that some motion of the tool did occur during the pin penetration. This can be eliminated by fastening the tool to the workpiece. This would have only second order effects on the drivepin velocity. That is, it would only change the amount of force exerted on the piston in proportion to the change in volume of the chamber. In actual operation, the volume of the chamber is determined by the sum of motion of the piston downward and the motion

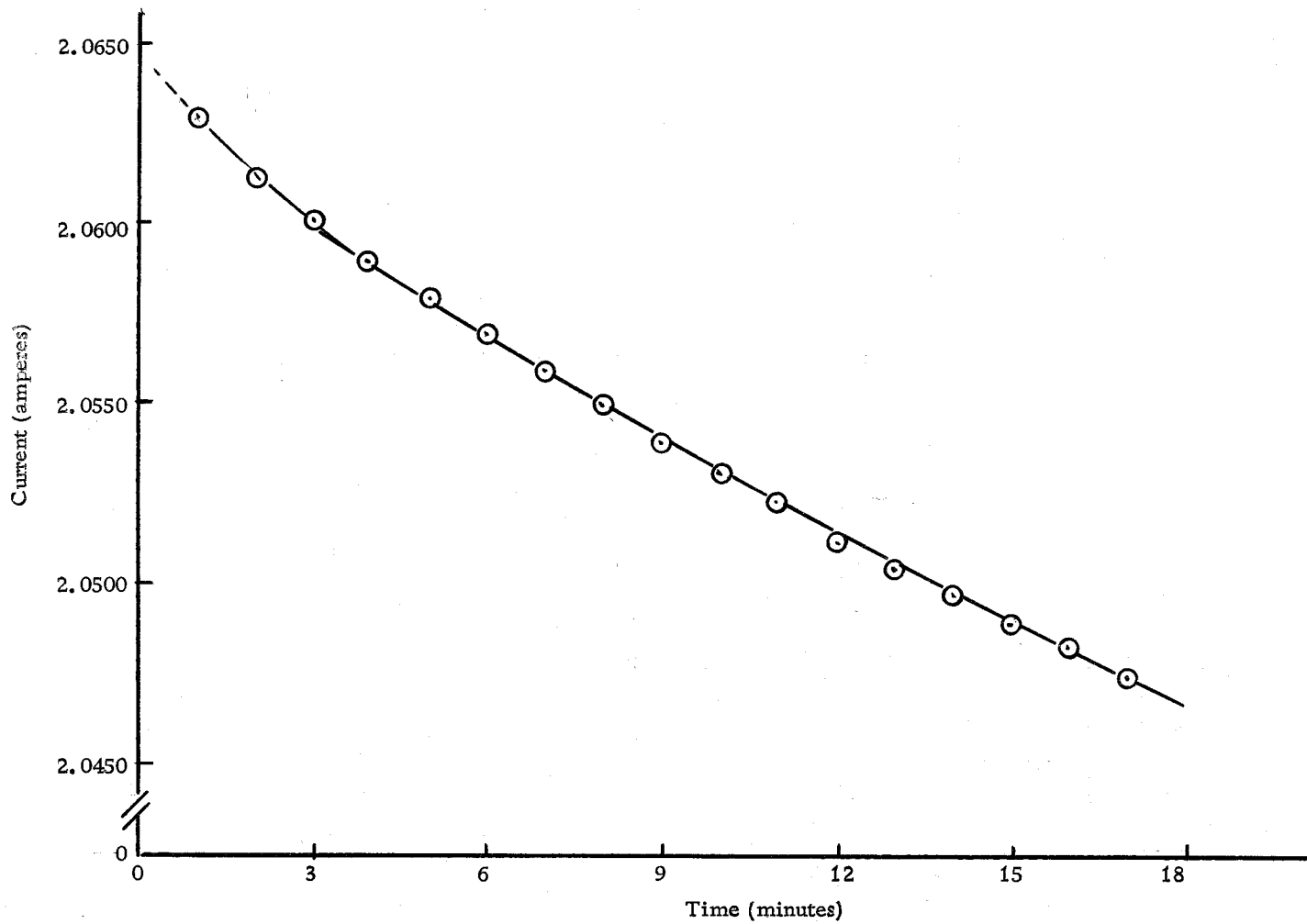


Figure 38. Variation of source current with time



of the tool upward. If the upward motion is restricted, the pressure on the piston will be increased. Or, the effect of the tool motion could be ignored since the tool velocity is much less than that of the drivepin. The equations of motion of the powder actuated tool and piston are shown in Appendix II. These calculations show the tool motion which could be expected for any given chamber pressure profile. It is also useful in understanding the nature of the forces effecting the tool bounce.

Another method of satisfying the fourth requirement would be to mount another potentiometer to measure the tool velocity with respect to the workpiece and algebraically add this output to the previous output. Thus the true drivepin velocity with respect to the workpiece can be determined by using the following rule for relative velocities:

$$V_A = V_B + V_{A/B}$$

where

$V_A$  = Velocity of the drivepin with respect to the workpiece

$V_B$  = Velocity of the tool with respect to the workpiece.

$V_{A/B}$  = Velocity of the drivepin with respect to the tool.

This test with a second potentiometer was planned but not accomplished because of the delay caused by the damaged elements.

These requirements, with the exception of the tool velocity, were met within the necessary limits so that the position versus

time data obtained can be considered a faithful reproduction of the actual phenomena. This information in itself, however, is not the final aim of this work since the drivepin acceleration is the real information required. Since the position information is continuous, the velocity and acceleration can be easily obtained graphically. The instantaneous velocity was determined in this manner by dividing the position versus time plot (photographs of the oscilloscope trace) into equal segments and measuring the slope for each interval with a drafting machine. This slope, multiplied by the proper scale factors, is equal to the average velocity in that interval. As the length of the intervals is reduced, it can be seen that the plot of these average velocities approaches a plot of the instantaneous velocity, and this process can be repeated to obtain the instantaneous acceleration. Figure 39 shows the range of velocities observed versus time. These velocities were obtained from the photographs of the traces or shown in Tables I and II.

A more sophisticated method called numerical differentiation is available for determining the acceleration from the position versus time data. The basic idea in numerical differentiation is to approximate the given function  $y = f(x)$  over a short range of  $x$  by a polynomial  $P_n(x)$  and then to differentiate that polynomial rather than the function  $f(x)$ . If  $f(x)$  is in the form of tabulated data, the polynomial  $P_n(x)$  is just the polynomial used in interpolation. This polynomial, obviously, can easily be differentiated (4, p. 125).

This polynomial or Newton-Gregory interpolation formula  $P_n(x)$  is given by the following formula:

Table I. Data Reduction--Vertical Sensitivity

1. Photo Number	A-1	B-1	B-2	B-3	B-4	C-1	C-2	C-3	C-4	D-1	D-2
2. H1 (inches)	2.075	1.350	1.575	1.575	1.575	1.575	1.575	1.575	1.575	1.575	1.575
3. H2 (inches)	.700	.075	.075	.075	.620	.430	.320	.350	.430	.360	.550
4. H1 - H2 (inches) (2-3)	1.375	1.275	1.500	1.500	.955	1.145	1.255	1.225	1.145	1.215	1.025
5. y1 (div)	+4.1	+4.8	+4.5	+4.6	+4.3	+3.7	+3.9	+3.8	+3.6	+4.8	+4.7
6. y2 (div)	-1.5	--	--	--	+0.8	-2.2	-2.5	-2.5	-2.2	-1.4	-0.6
7. y1 - y2 (div) (5-6)	5.6	--	--	--	3.5	5.9	6.4	6.3	5.8	6.2	5.3
8. Vert. Sens. $\frac{\text{inches}}{\text{div}} \frac{4}{7}$	(.246) .25	--	--	--	(.272) .27	(.194) .19	(.196) .20	(.194) .19	(.197) .20	(.196) .20	(.194) .19
Calibration Check											
9. Scope Vert. Scale Factor $\frac{\text{mv}}{\text{div}}$	--	50	50	50	100	50	50	50	50	50	50
10. Transducer Calibration $\frac{\text{mv}}{\text{div}}$	--	325	325	325	325	258	258	258	258	258	258
11. Calib. Vert. Sens. $\frac{\text{inches}}{\text{div}} \frac{9}{10}$	--	.154	.154	.154	.308	.194	.194	.194	.194	.194	.194

Table 2. Photo C-2 Typical Data Reduction--Velocity

Scope Abscissa (x div)	Time of Penetration (ms)	Average Slope (degrees)	$\frac{x \text{ div}}{y \text{ div}}$ Tan	Vert. Sens.* $\frac{\text{in.}}{y \text{ div}}$	Hor. Sens. $\frac{\text{ms}}{x \text{ div}}$	Sens. Mult. (x div)(5/6)	Av. Velocity (in./ms)(4 x 7)	Av. Velocity (in./sec.)	Av. Velocity FPS	$\frac{H \text{ (Inch)}}{(9 \times \text{Interval})}$	H1 - H2 (in.) (From Table 1)	% Error
-5												
-4												
-3	0.08	-52.5°	1.304	0.196	0.1	1.96	2.56	2560	214	0.0205		
-2	0.18	-53.2°	1.34	0.196	0.1	1.96	2.62	2620	218	0.0262		
-1	0.28	-52.3°	1.29	0.196	0.1	1.96	2.53	2530	221	0.0253		
0	0.38	-49.2°	1.16	0.196	0.1	1.96	2.27	2270	189	0.0227		
+1	0.48	-45.0°	1.00	0.196	0.1	1.96	1.96	1960	163	0.0196		
+2	0.58	-30.0°	0.577	0.196	0.1	1.96	1.13	1130	94	0.0113		
+3	0.68	-15.0°	0.268	0.196	0.1	1.96	0.525	525	44	0.0052		
+4	0.78	0.0°	0	0.196	0.1	1.96	0	0	0			
+5	0.88	0.0°	0	0.196	0.1	1.96	0	0				
										$\Sigma H = 0.1308$	1.255	4

\*From Table 1

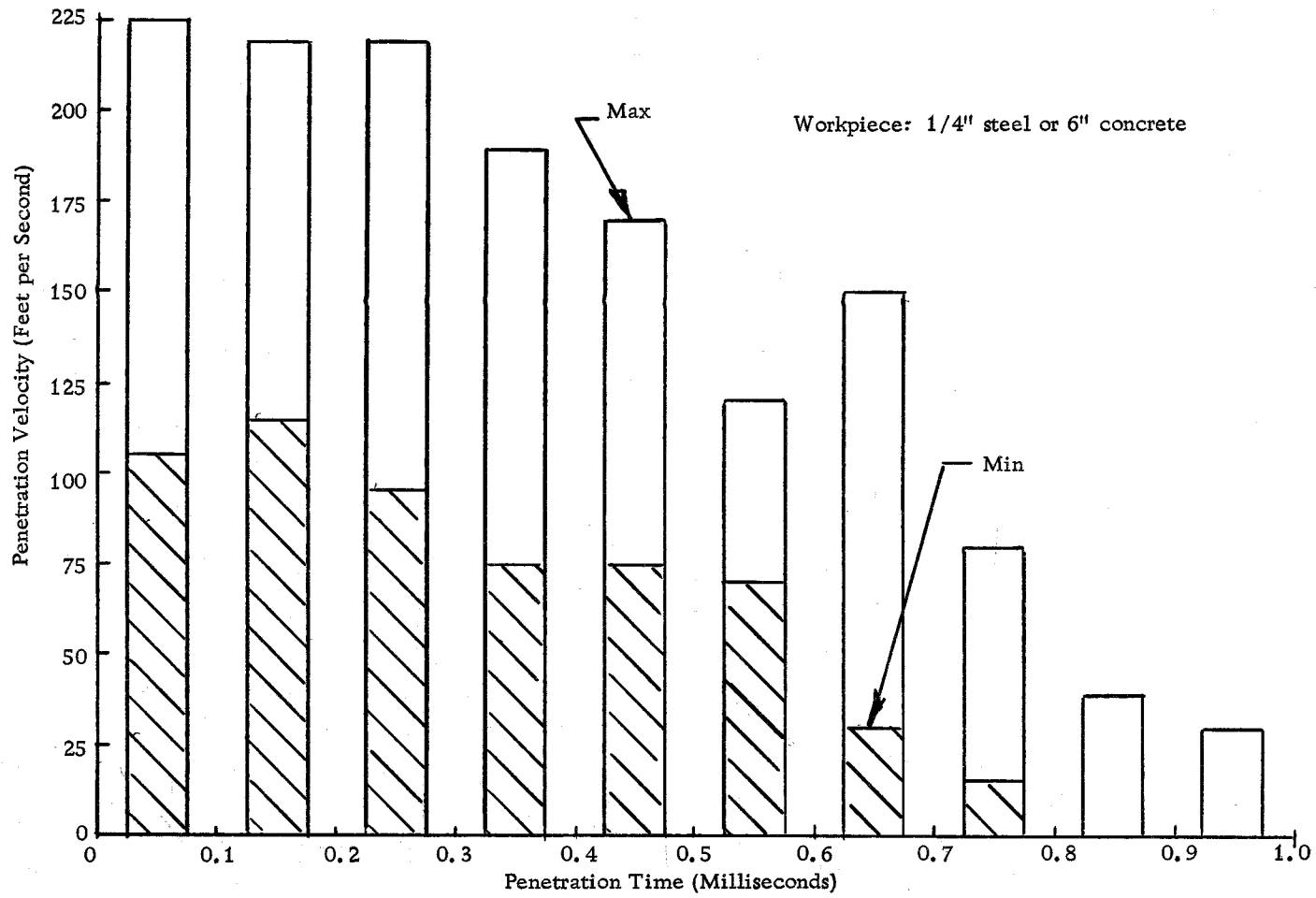


Figure 39. Penetration velocity vs. time

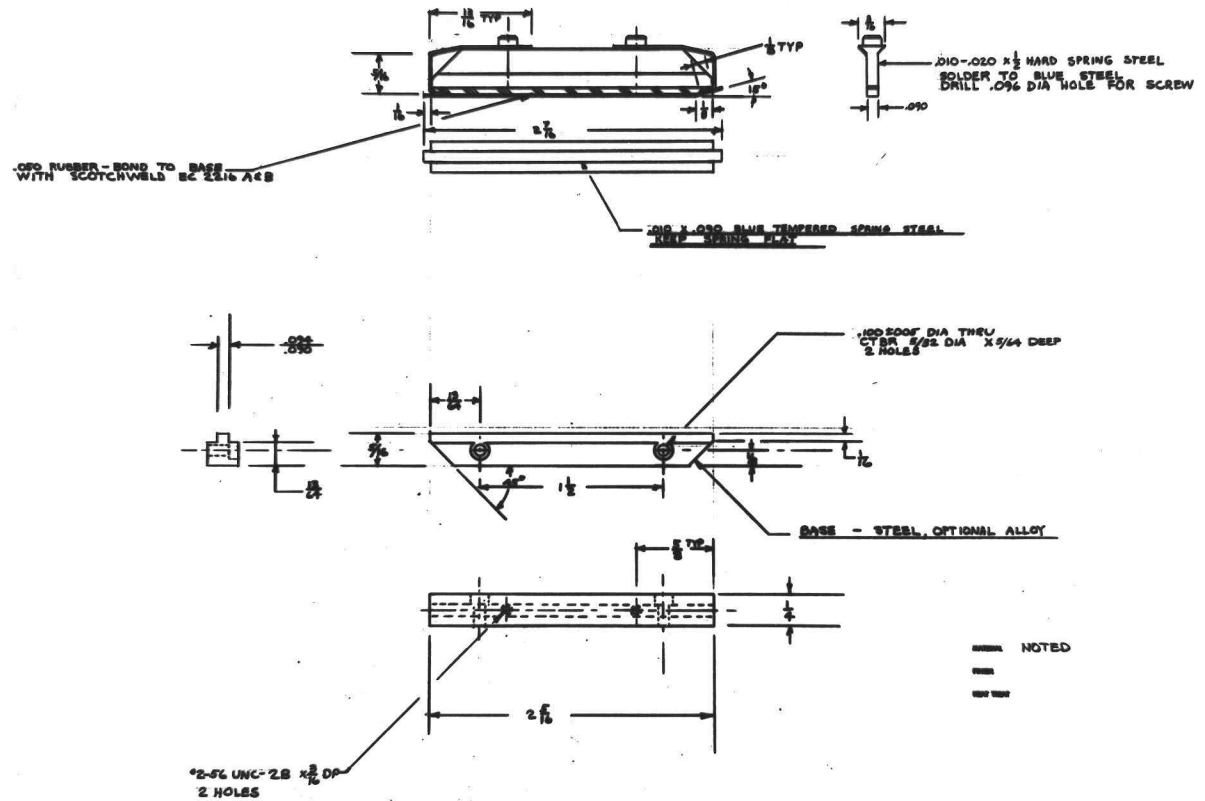


Figure 40. Collector 20-5

$$P_n(x) = f(a) + \frac{(x-a)}{h} \Delta f(a) + \frac{(x-a)[x-(a+h)]}{h^2 2!} \Delta^2 f(a) + \dots$$

$$+ \frac{(x-a)[x-(a+h)] \dots [x-(a+(n-1)h)]}{h^n n!} \Delta^n f(a)$$

where

$P_n(x)$  = the interpolating polynomial of degree  $n$

$f(a)$  = the value of the tabulated data at  $x = a$

$h$  = length of the interval between successive values of  $x$  of the tabulated data. Note: this method requires that the values of the data be equally spaced along the  $x$  axis; but there are methods for numerical differentiation where the ordinates are not equally spaced (4, p. 132).

$$\Delta f(a) = f(a+h) - f(a) = \text{differences of } f(a)$$

and the second difference

$$\Delta^2 f(a) = \Delta f(a+h) - \Delta f(a) = [f(a+2h) - f(a+h)] - [f(a+h) - f(a)]$$

and the  $n$ th difference of  $f(a)$  is

$$\Delta^n f(a) = f(a+nh) - n f[a+(n-1)h] + \frac{n(n-1)}{2!} f[a+(n-2)h] + \dots$$

$$+ (-1)^n f(a)$$

This formula is exact if the tabulated data is generated from a polynomial of degree  $n$  within  $n+1$  ordinates specified. This is true

no matter what value of  $x$  we choose (2, p. 253-256).

It is obvious that the coefficients of the polynomial will be different if the data is not exact depending on where the polynomial is evaluated. If, however, the polynomial is evaluated at the first value of  $x$  of the tabulated data of  $n + 1$  values, then a polynomial  $P_n(x)$  can be written which will approximate the tabulated function up to the  $n$ th degree term.

In general the accuracy increases with an increase of the degree  $n$  of the polynomial until a certain maximum accuracy is achieved. Beyond this point no appreciable increase in accuracy is obtained by an increase in  $n$  because of the effect of errors in the tabulated values of  $y$ . This maximum practical value of  $n$  is usually equal to the order of the most nearly constant difference column. The relative error in the derivative is usually considerably larger than the errors in the tabulated values of  $y$ . The higher derivatives can be obtained in a similar way, but the error in their evaluation increases with their order (4, p. 126).

To show how convenient this technique is for use with tabulated data, consider the following example:

$x$	$f(x)$	$\Delta f(x)$	$\Delta^2 f(x)$	$\Delta^3 f(x)$
0	2			
1	4	2		
2	4	0	-2	0
3	2	-2	-2	0
4	-2	-4	-2	0
5	-8	-6		



So the value of the polynomial at  $x = 0$  and  $h = 1$  is

$$P_n(0) = 2 + 2x - \frac{2(x)(x-1)}{2} = 2 + 3x - x^2$$

This also shows that since the second difference column is constant, further work may not be necessary.

Thus, if the value of the pin position were taken every one half division from the photographs of the oscilloscope trace, the polynomial  $P_n(x)$  can be evaluated at  $x = 0$ . Changing the independent variable  $x$  from the previous discussion to  $t$  for time and letting  $x = t$  and  $h = 1/2$  division:

$$\begin{aligned} \left[ P_{20}(t) \right]_{t=0} &= f(0) + \frac{x}{h} \Delta f(0) + \frac{x(x-h)}{h^2 2!} \Delta^2 f(0) + \frac{x(x-h)(x-2h)}{h^3 3!} \Delta^3 f(0) + \\ &\dots + \frac{x(x-h)(x-2h)\dots(x-19h)}{h^{20} 20!} \Delta^{20} f(0) \end{aligned}$$

This would result in a polynomial of the form

$$P_{20}(t) = a_0 + a_1 x + a_2 x^2 + a_3 x^3 + a_4 x^4 + \dots + a_{20} x^{20}$$

which is easily differentiated. This 20th degree polynomial could be easily evaluated on a digital computer.

It should be noted also, that  $P_n(t)$  is not unique even though every term in one of the difference columns is exactly zero.  $P_n(t)$  is only a polynomial which passes through the tabulated points. Any number of other functions of  $t$  could be found which pass through

these same points (4, p. 52-53).

These tabulated points, since they come from experimental data, are subject to random errors. Since these errors are greater in the derivatives than in the experimental data, it is desirable to find an approximating polynomial,  $P_n(t)$ , which reflects the general trend of the data without reproducing local fluctuations. The method of curve fitting by the method of Least Squares is designed to predict values of a function such that the sum (or integral) of the squares of the differences between the curve and the data will be a minimum (2, p. 230).

If  $n + 1$  pairs of values,  $(t_0, y_0)$ ,  $(t_1, y_1)$ ,  $(t_2, y_2)$ ,  $\dots$ ,  $(t_n, y_n)$ , are taken from the photograph of the trace (not necessarily at equal intervals), then an approximating polynomial  $P_m(t)$  can be written of degree  $m$  where  $m$  is less than  $n$ ,

$$P_m(t) = a_0 + a_1 t + a_2 t^2 + a_3 t^3 + \dots + a_m t^m.$$

If  $P_m(i)$  = the predicted value of the function at  $t = t_i$  and  $y_i$  is the observed value of the function at  $t = t_i$ ,

then the error is

$$e_i = P_m(i) - y_i$$

and the square of the error is

$$e_i^2 = \left[ P_m(i) - y_i \right]^2$$

and the sum of the squares of the error is

$$\begin{aligned}
 S &= \sum_{i=1}^n e_i^2 = \sum_{i=1}^n \left[ P_m(i) - y_i \right]^2 \\
 &= \sum_{i=1}^n \left[ a_0 + a_1 t_i + a_2 t_i^2 + a_3 t_i^3 + \dots + a_m t_i^m - y_i \right]^2
 \end{aligned}$$

To make  $S =$  a minimum, take the partial derivatives of  $S$  with respect to  $a_0, a_1, a_2, \dots, a_m$  and set these derivatives equal to zero. In this way  $m + 1$  equations can be written

$$s_0 a_0 + s_1 a_1 + s_2 a_2 + \dots + s_m a_m = v_0$$

$$s_1 a_0 + s_2 a_1 + s_3 a_2 + \dots + s_{m+1} a_m = v_1$$

.....

$$s_m a_0 + s_{m+1} a_1 + s_{m+2} a_2 + \dots + s_{2m} a_m = v_m$$

where

$$s_k = \sum_{j=0}^n t_j^k \quad \text{and} \quad v_k = \sum_{j=0}^n y_j t_j^k$$

(k = 0, 1, 2, 3, \dots, m)

These equations always have a unique solution for  $a_0, a_1, a_2, \dots, a_m$ ; and when these values are substituted into  $P_m(t)$ , the value of the sum of the squares  $S$  is actually a minimum (5, p. 243-244).

Therefore, these values of  $a_i$  substituted into  $P_m(t)$  yield the best fitting curve in the sense of Least Squares which represents

the tabulated data.

Up to this point in the discussion of curve fitting, approximating polynomials only were considered. However, this technique is just as valid if the function were linear, transcendental, or exponential. Since the method of Least Squares requires an estimate of the form of the best fitting curve or the required degree of the polynomial, sometimes considerable work can be saved by using another type function rather than evaluating the polynomial to a high degree to get the required fit.

The introduction of computers to this discussion brings up the question, why not feed the position data into an analog computer (operational amplifiers) and differentiate twice to obtain the drivepin acceleration? This would be quite reasonable except for practical problems associated with differentiation using an analog computer. Differentiation with an operational amplifier is not recommended for determination of velocity and acceleration because noise is amplified

(3). Murphy (6, p. 492) elaborates on this same subject:

Although it is possible to construct a differentiating component using a high-gain amplifier with a resistive feedback impedance  $R$  and a capacitive input impedance  $1/Cs$ , it is customary to avoid the use of differentiation in the use of the electronic analogue computer. One reason for using a differentiator only when its use cannot easily be avoided is that in general the derivative of a given signal contains higher-frequency sinusoidal components of appreciable amplitude than does the original signal itself; therefore, in order to obtain equivalent results it is necessary that amplifiers used with

differentiating components have a greater band-width than those required to solve the given problem when the use of differentiators is avoided. A second reason for avoiding the use of differentiating components is that the gain of a true differentiator rises at a rate of 20 decibels per decade, and, consequently, high-frequency noise is greatly amplified. Because there is no great need for a symbol for an electronic analogue computer differentiating component, no such symbol is given here.

## VI. CONCLUSIONS AND RECOMMENDATIONS

The final configuration of this method of measuring the instantaneous position of the drivepin consists of a battery energized slide wire potentiometer mounted inside a barrel extension.

The head of the drivepin contacts the slide wire during penetration and transfers this voltage to the collector. The collector transfers this voltage into an oscilloscope for display as a function of time. The external trigger signal for starting the display is obtained from the first motion of the drivepin as it passes through a metal foil on the surface of the base material.

This measuring system, together with mathematical techniques was shown to be an effective method of determining the drivepin instantaneous velocity and acceleration.

The method is simple, has a high frequency response, and is not expensive. The resistance element, however, has only marginal mechanical strength which will allow only approximately 20 firings per resistance element.

The following recommendations are offered for future models of this transducer:

1. Vulcanize the resistance element and collector to their rubber substrate.

2. Attach the resistance element such that two sides are bonded to the rubber and load the rubber in shear.
3. Select a harder, stronger, higher-resistance resistance element such as cobalt base or nickel base superalloys.
4. Reduce the diameter of the barrel of the transducer to provide a better guide for the head of the drivepin and reduce the amount of deflection required of the resistance element.
5. Investigate the elimination of the collector and the use of the barrel itself to transfer the voltage of the drivepin to the oscilloscope.

## BIBLIOGRAPHY

1. Buchbinder, Harold G. Precision potentiometers. *Systems Designer's Handbook* 8(1):21-50. January, 1964.
2. Gaskell, Robert E. *Engineering mathematics*. New York, Holt, Rinehart and Winston, 1958. 631 p.
3. Keller, Robert E. Analyzing mechanisms with an analog computer. *Machine Design* 37:153-158. October 28, 1965.
4. Kunz, Kaiser S. *Numerical analysis*. New York, McGraw Hill, 1957. 381 p.
5. Milne, William E. *Numerical calculus*. Princeton, Princeton University Press, 1949. 393 p.
6. Murphy, Gordon J. *Basic automatic control theory*. New York, Van Nostrand, 1957. 557 p.
7. Schoevitz, H. *Notes on linear variable differential transformers*. Camden, New Jersey, Schoevitz Engineering, 1955. 19 p.
8. Skilling, Hugh H. *Electrical engineering circuits*. New York, Wiley, 1957. 724 p.
9. Stein, Peter. Strain gage readings. *Instruments and Control Systems* 38:113-117. June, 1965.
10. Timoshenko, S. *Strength of materials*. 3d ed. Vol. 2. Princeton, Van Nostrand, 1956. 572 p.



APPENDICES

## APPENDIX I

Linearity and Frequency Response of a Potentiometer  
Measuring System

A potentiometer must be supplied by a constant current source in order to have a truly linear output (9). Since the supply current is made up of the current in the resistance element and the current in the load, the constant source current requirement is approached as the load current approaches zero. The following analysis shows the variation of the load current with wiper position and load impedance.

Figure 1 is a schematic diagram of the circuit showing the battery lead resistance and the load (oscilloscope).

Now for the circuit of Test F:

$$H = 0.06 \Omega$$

$$G = 0.18 \Omega$$

$$R = 0.31 \Omega$$

So for simplicity assume:

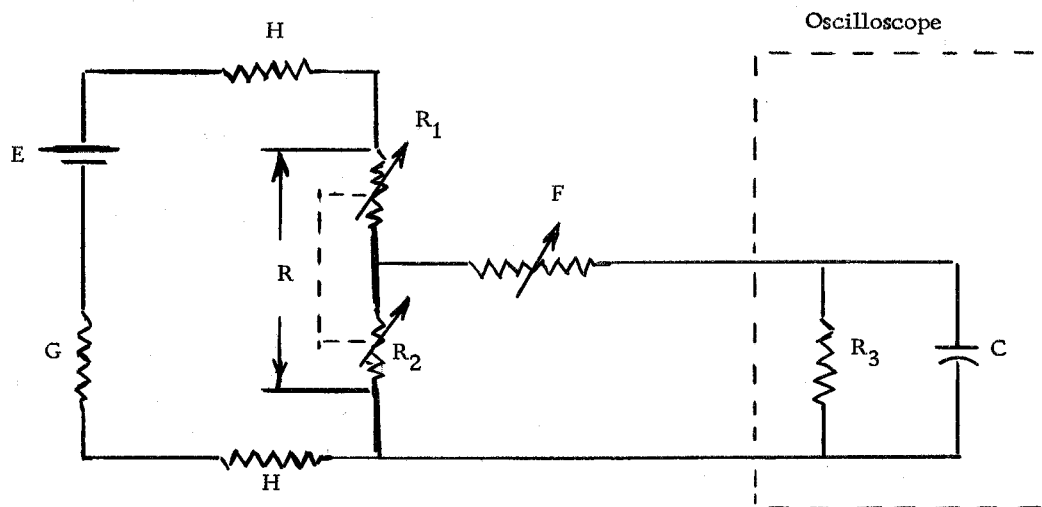
$$H = 0$$

$$G = 0$$

$$F = 0$$

and since  $R_2$  and  $R_3$  are in parallel and  $0 < R_2 < 0.31 \Omega$ , then the impedance of the pair will be

$$\frac{0.31(1 \times 10^6)}{0.31 + (1 \times 10^6)}$$



Where

$E$  = Battery voltage

$G$  = Battery impedance

$H$  = Battery lead impedance

$R_1$  = Resistance of the top of the resistance element

$R_2 = R - R_1$  = Resistance of bottom of the resistance element

$R$  = Total resistance of the element

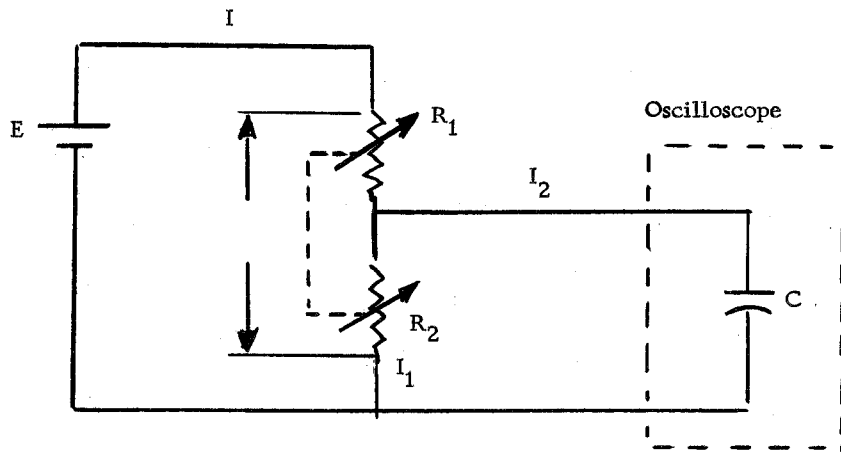
$F$  = Contact resistance of the drivepin

$R_3$  = Scope input resistance =  $1 \text{ M}\Omega$

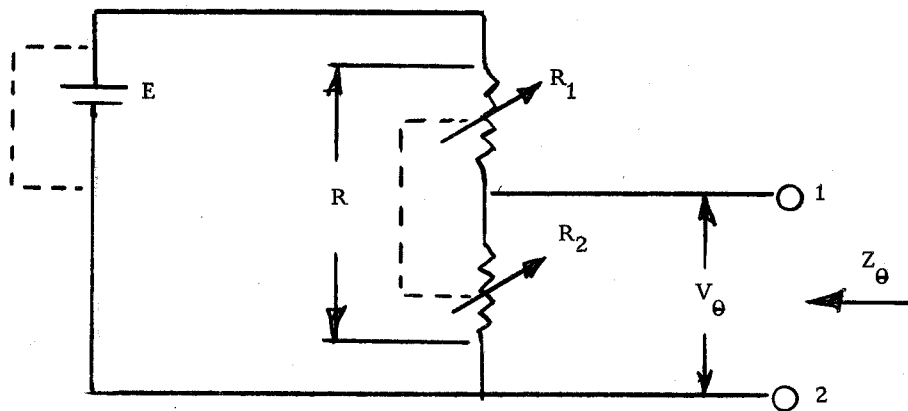
$C$  = Scope input capacitance =  $20 \text{ pf}$

The distributed inductance and capacitance were considered negligible.

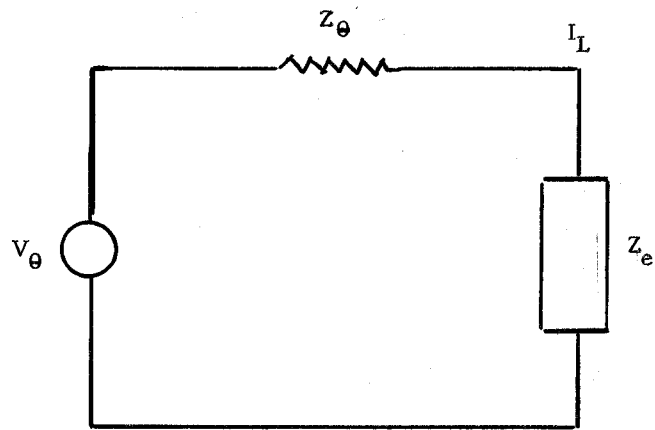
Appendix Figure 1. Potentiometer circuit



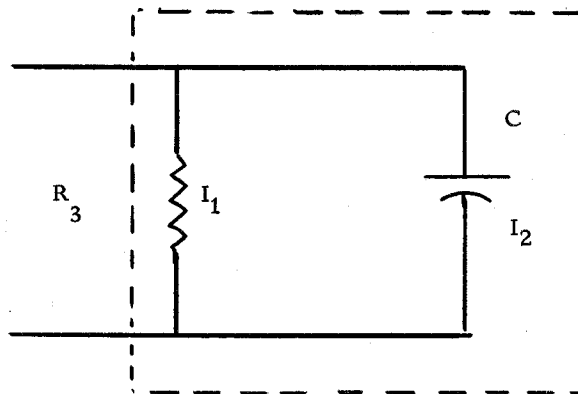
Appendix Figure 2. Simplified potentiometer circuit



Appendix Figure 3. Simplified transducer impedance



Appendix Figure 4. Thevenin's equivalent circuit



Appendix Figure 5. Oscilloscope input impedance

or  $0.31\Omega$ . So assume  $R_3 = \infty$

Then the new circuit will be shown in Figure 2.

$$E = R_1 I + R_2 I_1$$

$$I = I_1 + I_2$$

$$E = R_1 I + \frac{Q}{C}$$

and

$$\frac{dQ}{dt} = I_2$$

Taking the Laplace transforms of the above equations,

Note:  $L[I] = i(s) = i$  and  $L[Q] = q(s) = q$

$$i - i_1 - i_2 = 0$$

$$R_1 i + R_2 i_1 = \frac{E}{s}$$

$$R_1 i + \frac{1}{C} q = \frac{E}{s}$$

where

$$q = \frac{1}{s} \left[ i_2 + Q(0) \right]$$

so

$$R_1 i + \frac{1}{Cs} i_2 = \frac{E}{s} - \frac{Q(0)}{Cs}$$

Now let  $Q(0) = 0$  and construct the following augmented matrix with a check column with the above equations

$$\begin{array}{ccccc}
 & & & & * \\
 1 & -1 & -1 & 0 & -1 \\
 R_1 & +R_2 & 0 & \frac{E}{s} & R + \frac{E}{s} \\
 R_1 & 0 & \frac{1}{Cs} & \frac{E}{s} & R_1 + \frac{1}{Cs} + \frac{E}{s}
 \end{array}$$

\*Check Column = the sum of the coefficients of each row.

Now the following auxiliary matrix can be formed using the Crout method (4, p. 228, 229).

$$\begin{array}{cccccc}
 & & & & & ** \\
 1 & -1 & -1 & 0 & -1 & -2 \\
 R_1 & R & \frac{R_1}{R} & \frac{E}{sR} & \frac{1+R_1s+E}{sR} & \frac{R_1s+E}{sR} \\
 R_1 & R_1 & \frac{R+R_1R_2Cs}{CsR} & \frac{ER_2C}{R+R_1R_2Cs} & \frac{1+ER_2C}{R+R_1R_2Cs} & \frac{ER_2C}{R+R_1R_2Cs}
 \end{array}$$

\*\* Sum of the coefficients to the right of the diagonal, but not including the diagonal. This check column should be one less than the column to the left.

So

$$i_2 = \frac{ER_2C}{R+R_1R_2C}$$

or

$$i_2 = \frac{E}{R_1} \left[ \frac{1}{s + \frac{R}{R_1R_2C}} \right]$$

or

$$i_2 = \frac{E}{R_1} e^{-\frac{Rt}{R_1 R_2 C}}$$

Thus the time constant will vary with the wiper position by  $\frac{R_1 R_2}{R}$ . The time constant for  $R_1 = \frac{R}{4}$ ,  $\frac{R}{2}$ , and  $\frac{3R}{4}$  is  $\frac{3}{16} \frac{R}{C}$ ,  $\frac{3}{16} \frac{R}{C}$  respectively. But  $R = 0.31\Omega$  and  $C = 20 \times 10^{-12}$  farads so the time constant at  $\frac{R}{2}$  is  $4 \times 10^{-12}$  seconds.

Therefore, the current in  $I_2$ , the oscilloscope parallel capacitance, will drop nearly to zero in three time constants or approximately  $12 \times 10^{-12}$  seconds. Since the horizontal sensitivity of most of these tests was  $1 \times 10^{-4}$  seconds, it is obvious that the delay of  $12 \times 10^{-12}$  seconds would not be seen on the oscilloscope.

It can be seen from Figure 1 that the wiper contact resistance will tend to reduce the dc current in the oscilloscope circuit since it is in series with one megohm  $R_3$ . This will help the battery maintain a constant current. This same contact resistance, however, will increase the time constant for charging the 20 picofarad oscilloscope capacitance, but an increase of many orders of magnitude can be tolerated.

This same result can be quickly obtained by using Thévenin's electrical network theorem. Combining the series resistances of the potentiometer battery and cables, Thévenin's equivalent of the circuit of Figure 3 is:



$$V_{\theta} = \frac{ER_2}{R}$$

where  $V_{\theta}$  = open circuit voltage and

$$Z_{\theta} = \frac{R_1 R_2}{R}$$

where  $Z_{\theta}$  = impedance of the circuit with all voltage sources (8, p. 336-338). So Thévenin's equivalent of the complete circuit is shown in Figure 4.

So

$$I_L = \frac{V_{\theta}}{Z_{\theta} + Z_e} = \left[ \frac{ER_2}{R} \right] \left[ \frac{1}{\frac{R_1 R_2}{R} + Z_e} \right]$$

or

$$I_L = \frac{ER_2}{R_1 R_2 + Z_e(R)}$$

or

$$I_L \left[ R_1 R_2 + Z_e(R) \right] = ER_2$$

Now  $Z_e$  is the oscilloscope impedance and is shown in Figure 5.

Now taking the Laplace transform of the above equation,

$$i(s) = \frac{e(s)R_2}{R_1 R_2 + Z_e(s)R}$$

Now consider the current in  $R_3$  to be insignificant. Therefore

$R_3 = \infty$ . But  $Z_e(s)$  for a capacitor with initial charge  $Q(0)$  is

$$\frac{1}{Cs} \left[ 1 + \frac{Q(0)}{i(s)} \right]$$

If

$$Q(0) = 0$$

then

$$i(s) = \frac{e(s)R_2}{R_1R_2 + \frac{R}{Cs}}$$

where  $C$  is the capacitance in farads.

Then

$$i(s) = \frac{e(s)R_2Cs}{R_1R_2Cs + R} = \frac{se(s)}{R_1} \left[ \frac{1}{s + \frac{R}{R_1R_2C}} \right]$$

Now if

$$E = 0, \text{ at } t < 0$$

$$E = E, \text{ at } t > 0$$

then

$$e(s) = \frac{E}{s}$$

So

$$i(s) = \frac{E}{R_1} \left[ \frac{1}{s + \frac{R}{R_1R_2C}} \right]$$

and the inverse of  $i(s)$  is

$$I(t) = \frac{E}{R_1} e^{-\frac{Rt}{R_1R_2C}}$$

which is the same as the equation for  $I_2$ .

The conditions which must be met for Thévenin's Theorem to be valid are

1.  $Z_{\theta}$  may be a network of anything. Sources may be either constant-current or constant voltage.
2. Impedances are linear.
3.  $Z_e$  can be a single impedance, or it can be the input impedance to a passive or active network of any degree complication.\*

These were all met in this circuit.

This, then, shows the magnitude of the wiper current  $I_2$  as a function of time and frequency for the test potentiometer circuit (assuming the oscilloscope resistance  $R_3$  to be infinite).

---

\* Thévenin's equivalent is equivalent at the terminals,  $Z_{\theta}$ , and in the external circuit, but not at all within the original network (8, p. 336-338).

## APPENDIX II

## Equation of Motion of the Powder Actuated Tool and Piston

The equations of motion for the tool and piston are of interest for determining the actual motion of the tool during pin penetration. The transducer developed in the body of the thesis measures the drivepin position with respect to the tool, but the parameter desired is the drivepin position with respect to the workpiece. Consequently, these equations are derived to show the time and nature of tool motion.

A schematic of the system is shown in Figure 6. Now a free body diagram of the tool, Figure 7, shows that three forces act on the tool, the force of the operator  $P$ , the force,  $F(t)$ , generated by the gas pressure, and the reaction,  $R$ , on the workpiece. This  $F(t)$  is not known so the mathematical treatment will consider this to be any function of time.

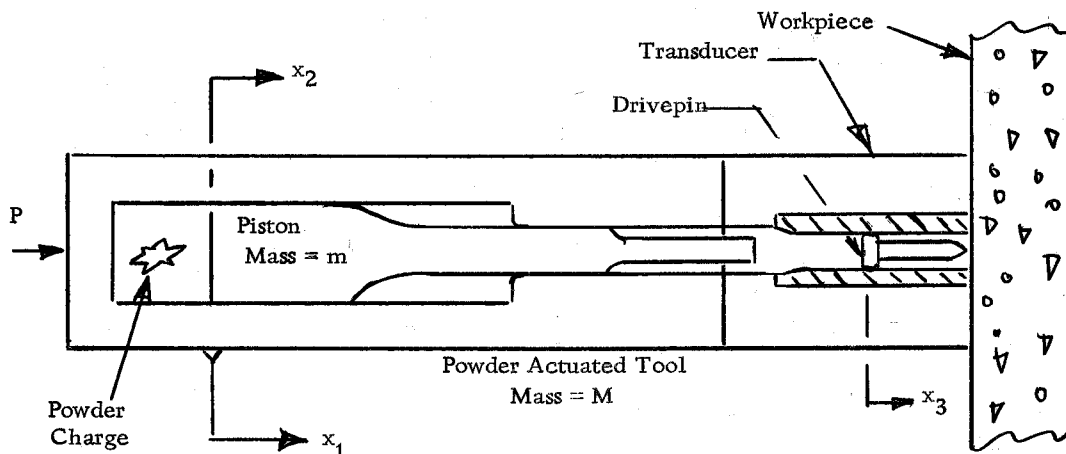
Summing the forces in Figure 7 and setting them equal to the mass times the acceleration yields

$$M\ddot{x}_1 = P - R - F(t)$$

where

$$\ddot{x}_1 = \frac{d^2 x_1}{dt^2}$$

Note that  $R = P - F(t)$ . That is, the reaction on the workpiece is the operator force, which is assumed to be constant, minus the force of

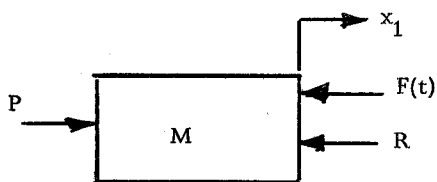


Where

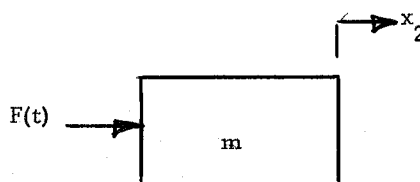
- $P$  = Force applied by the operator  
(must be 35 at time of firing)
- $x_1$  = Position of the tool
- $x_2$  = Position of the piston
- $x_3$  = Position of the drivepin
- $M$  = Mass of the tool without piston and transducer
- $m$  = Mass of the piston

Ignore gravity forces and friction forces of the power plug fingers on the piston and transducer contact force on the drivepin.

Appendix Figure 6. Powder actuated tool and piston



Appendix Figure 7. Free body diagram of the tool.



Appendix Figure 8. Free body diagram of the piston

the gas pressure. This reaction is equal to  $P - F(t)$  as long as the tool is touching the workpiece, but  $R$  is zero as soon as  $x_1$  is negative or as soon as the tool bounces. Let the time the tool starts in the negative direction be  $k$ .

Then

$$R = \begin{cases} P - F(t) & 0 < t < k \\ 0 & t > k \end{cases}$$

Taking the Laplace transform of the first equation yields

$$M \left[ s^2 x_1(s) - s x_1(0) - \dot{x}_1(0) \right] = \frac{P}{s} - f(s) - \int_0^k e^{-st} [P - F(t)] dt \\ - \int_k^\infty e^{-st} [P - F(t)] dt$$

But

$$[P - F(t)] = 0 \text{ for } k < t < \infty$$

and

$$x_1(0) = \ddot{x}_1(0) = 0$$

$$\dot{x}_1(0) = \frac{dx_1}{dt}$$

so the above equation reduces to

$$Ms^2 x_1(s) = \frac{P}{s} - f(s) - \int_0^k e^{-st} [P - F(t)] dt$$

or

$$Ms^2 x_1(s) = \frac{P}{s} - f(s) - P \left[ \frac{e^{-st}}{-s} \right]_0^k + \int_0^k e^{-st} F(t) dt$$

so

$$x_1(s) = \frac{P}{M} \frac{e^{-ks}}{s^3} + \frac{1}{Ms^2} \int_0^k e^{-st} F(t) dt - \frac{1}{M} \frac{f(s)}{s^2}$$

where

$$f(s) = \text{Laplace transform of } F(t)$$

$$x_1(s) = \text{Laplace transform of } x_1(t)$$

Now, some knowledge of  $F(t)$  must be known. Assume  $F(t) = A$ ,

then

$$f(s) = \frac{A}{s}$$

Substituting these gives:

$$x_1(s) = \frac{Pe^{-ks}}{Ms^3} + \frac{A}{Ms^2} \int_0^k e^{-st} dt - \frac{A}{Ms^3}$$

or

$$x_1(s) = \frac{Pe^{-ks}}{Ms^3} + \frac{A}{Ms^2} \left[ \frac{e^{-st}}{-s} \right]_0^k - \frac{A}{Ms^3}$$

$$x_1(s) = \frac{Pe^{-ks}}{Ms^3} - \frac{Ae^{-ks}}{Ms^3} + \frac{A}{Ms^3} - \frac{A}{Ms^3}$$

or

$$x_1(s) = \left[ \frac{P - A}{M} \right] \frac{e^{-ks}}{s^3}$$

so

$$x_1(t) = \left[ \frac{P - A}{M} \right] \begin{cases} 0 & \text{when } 0 < t < k \\ \frac{(t-k)^2}{\Gamma(3)} & \text{when } t > k \end{cases}$$

But

$$\Gamma(k+1) = \int_0^{\infty} x^k e^{-x} dx = k! \quad (\text{when } k \text{ is a positive integer})$$

and

$$\Gamma(3) = \int_0^{\infty} x^2 e^{-x} dx = 2$$

so

$$x_1(t) = \left[ \frac{P - A}{M} \right] \begin{cases} 0 & \text{when } 0 < t < k \\ \frac{(t-k)^2}{2} & \text{when } t > k \end{cases}$$

But  $k$  is the time  $x_2(t)$  goes negative. This says that if the pressure in the chamber is constant  $A$ , the motion of the tool will start whenever  $A$  is greater than  $P$ .

For

$$A > P$$

$$x_1(t) = \frac{P - A}{M} \frac{t^2}{2} \quad \text{which is the familiar form } 1/2 at^2$$

where

$$a = \frac{F}{M} \quad \text{from Newton's Law}$$

At the same time  $F(t)$  acts on the tool, it also acts on the piston;

so from Figure 8

$$F(t) = m\ddot{x}_2$$



and

$$\ddot{x}_2 = \frac{F(t)}{m}$$

Then

$$s^2 x_2(s) - s x_2(0) - \dot{x}_2(0) = \frac{f(s)}{m}$$

again let

$$x_2(0) = \dot{x}_2(0) = 0$$

so

$$x_2(s) = \frac{f(s)}{ms^2}$$

Now, if

$$F(t) = A$$

then

$$x_2(s) = \frac{A}{m} \frac{1}{s^3}$$

and

$$x_2(t) = \frac{A}{m} \frac{t^2}{2}$$

Now the piston must travel a certain distance before it contacts the drivepin. Consequently, the force  $F(t)$  tending to make the tool bounce always occurs before the drivepin motion starts. This, then, gives the tool a better chance to bounce during the drivepin motion, and it will bounce any time  $A$  is greater than  $P$ .

## APPENDIX III

Test Description A

Date: 12-9-65

Time: 1000

Operator: P.J.

Test Circuit Number: 1

Base Material Description Number: 1    Total Shots Fired: 4

Tool Type: 110

S/N: 36124

Load: s3, P/N 65396

Piston Number: 66025

## Camera

Type C 12

S/N Omark: 3397

Polaroid Film: 3000 speed/Type 47 Shutter: T

f stop: 4

## Oscilloscope

Tektronix Type 536

S/N: Omark 2921

Vertical Plug-in Amplifier: 1A1

S/N: Omark 5389

Horizontal Plug-in Amplifier: T

S/N: 01505-104

Vertical Amplifier (Type 1A1) Controls:

Channel 1

Channel 2

Input Selector: dc    Mode: Ch. 1    Input Selector: GRND

Volts/cm (see Data Sheet): Calibrated

Horizontal Amplifier (Type "T") Controls:

Triggering Mode: dc

Triggering Level: three o'clock

Stability: Preset

Time/div (see Data Sheet): Calibrated

Sweep: Normal 5x Magnifier: Off Triggering Slope: minus EXTERNAL

## APPENDIX IV

Test Description B

Date: 1-19-66

Time: 0815

Operator: P.J.

Test Circuit Number: 2

Base Material Description Number: 1

Total Shots Fired: 12

Tool Type: 110

S/N: 36124

Load: s3, P/N 65396

Piston Number: 20-4-3-A (5-7/8")

## Camera

Type C 12

S/N: Omark 3397

Polaroid Film: 3000 speed/Type 47

f stop: 4

## Oscilloscope

Tektronix Type 536

S/N: Omark 2921

Vertical Plug-in Amplifier: CA

S/N: 06331

Horizontal Plug-in Amplifier: T

S/N: 01505-104

Vertical Amplifier (Type CA) Controls:

Channel A: dc

Mode: A only

Volts/cm (see Data Sheet): Calibrated

Polarity: Plus

Horizontal Amplifier (Type T) Controls:

Triggering Mode: dc

Triggering Level: three o'clock

Stability: Preset

Time/div (see Data Sheet): Calibrated

Sweep: Single

Triggering Slope: minus EXTERNAL

5x Magnifier: Off

## APPENDIX V

Test Description C

Date: 2-2-66

Time: 0830

Operator: P. J.

Test Circuit Number: 3

Base Material Description Number: 2

Total Shots Fired: 10

Tool Type: 110

S/N: 36124

Load: s3, P/N 65396

Piston Number: 20-4-3-A (5-7/8")

## Camera

Type C 12, Shutter T

S/N: Omark 3397

Polaroid Film: 3000 speed/Type 47

f stop: 4

## Oscilloscope

Tektronix Type 536

S/N: Omark 2921

Vertical Plug-in Amplifier: CA

S/N: 06331

Horizontal Plug-in Amplifier: T

S/N: 01505-104

Vertical Amplifier (Type CA) Controls:

Channel A: dc

Mode: A only

Volts/cm (see Data Sheet): Calibrated

Polarity: Plus

Horizontal Amplifier (Type "T") Controls:

Triggering Mode: dc

Triggering Level: 12:15 o'clock

Stability: Preset

Time/div (see Data Sheet): Calibrated

Sweep: Single

Triggering Slope: plus EXTERNAL

5x Magnifier: Off

## APPENDIX VI

Test Description D

Date: 2-8-66

Time: 0830

Operator: P.J.

Test Circuit Number: 4

Base Material Description Number: 2

Total Shots Fired: 3

Tool Type: 110

S/N: 36124

Load: s3, P/N 65396

Piston Number: 20-4-3-A (5-7/8")

## Camera

Type C 12, Shutter T

S/N: Omark 3397

Polaroid Film: 3000 speed/Type 47

f stop: 4

## Oscilloscope

Tektronix Type 536

S/N: Omark 2921

Vertical Plug-in Amplifier: CA

S/N: 06331

Horizontal Plug-in Amplifier: T

S/N: 01505-104

Vertical Amplifier (Type CA) Controls:

Channel A: dc

Mode: A only

Volts/cm (see Data Sheet): Calibrated

Polarity: Plus

Horizontal Amplifier (Type "T") Controls:

Triggering Mode: dc

Triggering Level: 12:15 o'clock

Stability: Preset

Time/div (see Data Sheet): Calibrated

Sweep: Single

Triggering Slope: plus EXTERNAL

5x Magnifier: Off

## APPENDIX VII

Test Description E

Date: 3-7-66

Time: 1700

Operator: P.J.

Test Circuit Number: 5

Base Material Description Number: 3

Total Shots Fired: 6

Tool Type: 110

S/N: 36124

Load: s3, P/N 65396

Piston Number: 20-4-3-A (5-7/8")

## Camera

Type C 12, Shutter T

S/N: Omark 3397

Polaroid Film: 3000 speed/Type 47

f stop: 2.8

## Oscilloscope

Tektronix Type 551

S/N: Omark 3396

Vertical Plug-in Amplifier: CA (upper beam)

S/N: 06331

Vertical Plug-in Amplifier: 1A1 (lower beam)

S/N: Omark 5389

Vertical Amplifier (Type CA) Controls: (upper beam)

Channel A: dc

Mode: A only

Volts/cm (see Data Sheet): Calibrated

Polarity: plus

Vertical Amplifier (Type 1A1) Controls: (lower beam)

Channel 1: Input Selector: dc

Channel 2 Input Selector: GRND

Volts/cm (see Data Sheet): Calibrated

Mode: Channel 1

Horizontal Internal Amplifier Controls:

Triggering Mode: dc

Triggering Level: 2:30 o'clock

Stability: Preset

Time/div (see Data Sheet): Calibrated

Single Sweep: In

Triggering Slope: plus EXTERNAL

Horizontal Display: Normal

Trigger Range: divided by 10

## APPENDIX VIII

Test Description F

Date: 3-8-66

Time: 1900

Operator: P. J.

Test Circuit Number: 6

Base Material Description Number: 3

Total Shots Fired: 5

Tool Type: 110

S/N: 36124

Load: s3, P/N 65396

Piston Number: 20-4-3-A (5-7/8")

## Camera

Type C 12, Shutter T

S/N: Omark 3397

Polaroid Film: 3000 speed/Type 47

f stop: 4

## Oscilloscope

Tektronix Type 536

S/N: Omark 2921

Vertical Plug-in Amplifier: CA

S/N: 06331

Horizontal Plug-in Amplifier: T

S/N: 01505-104

Vertical Amplifier (Type CA) Controls:

Channel A: dc

Channel B: dc

Volts/cm (see Data Sheet): Calibrated

Volts/cm (see Data Sheet): Calibrated

Polarity: Plus

Polarity: Plus

Mode: Chopped

Horizontal Amplifier (Type "T") Controls:

Triggering Mode: dc

Triggering Level: one o'clock

Stability: Preset

Time/div (see Data Sheet): Calibrated

Sweep: Single

Triggering Slope: Plus EXTERNAL

5x Magnifier: Off